

V. THEORETICAL PHYSICS

OVERVIEW

Theoretical research in the Physics Division addresses a broad range of problems involving the structure and dynamics of hadrons and nuclei. There is a strong emphasis on comparison to data from Argonne's ATLAS facility, TJNAF, and other laboratories around the world. Our work includes the modeling and application of quantum chromodynamics to light- and heavy-hadron structure at zero temperature and density, and at the extremes of temperature and density appropriate to the early universe, neutron stars, and upcoming RHIC and LHC experiments. We develop reaction theories for meson and nucleon-resonance production experiments at JLab, and for medium effects on mesons and resonances in nuclei and dense matter also relevant to RHIC. We construct realistic two- and three-nucleon potentials that give accurate fits to NN elastic scattering data and trinucleon properties, and use them in detailed many-body calculations of light and closed-shell nuclei, nuclear matter and neutron stars, and in a variety of astrophysically important electroweak reactions. Our nuclear structure and reaction studies include coupled-channels calculations of heavy-ion reactions near the Coulomb barrier, and calculations of observables in breakup reactions of nuclei far from stability. We also study high-spin superdeformation, spectroscopy of the heaviest elements ($A \approx 250$), and nuclear structure near the proton-drip line. Additional research is made in atomic physics, neutron physics, quantum computing and fundamental quantum mechanics. Several of our projects involve major numerical simulations using the massively parallel computer systems at Argonne and NERSC.

A. NUCLEAR DYNAMICS WITH SUBNUCLEONIC DEGREES OF FREEDOM

The objective of this research program is to investigate the role of mesons, nucleon resonances, and quark-gluon degrees of freedom in nuclear dynamics.

The Dyson-Schwinger equations (DSEs) provide a nonperturbative approach to studying the continuum formulation of QCD, making accessible phenomena such as confinement, dynamical chiral symmetry breaking, and bound state structure and interactions. However, they also provide a generating tool for perturbation theory and hence their application is tightly constrained at high-energy. This is the particular feature of the phenomenological application of DSEs: their ability to furnish a unified description of high- and low-energy phenomena in QCD. This last year has seen many successful applications. For example, we developed a Faddeev amplitude model of the nucleon, and used it to calculate a wide range of leptonic and nonleptonic nucleon couplings and form factors, demonstrating that soft form factors are the natural outcome of quark substructure. We demonstrated that scalar and pseudoscalar bound states persist into the quark gluon plasma and that their widths remain large until very near the critical temperature for plasma formation. We also explored the consequences that non-Markovian effects in the quantum Vlasov equation's source term can have on the evolution to equilibrium of particles produced in an ultrarelativistic heavy ion collision.

At the level of meson and nucleon resonance degrees of freedom, we have developed a dynamical model for relating the structure of nucleon resonances (N^*) as predicted by various QCD-based hadron models to the data on N and N reactions. The model has been used to test constituent quark models and to extract the Q^2 -dependence of transition factors from the recent data obtained at TJNAF, Mainz, and MIT-Bates. The amplitudes of vector meson photoproduction at a few GeV were analyzed based on the diffractive Pomeron-exchange and meson-exchange mechanisms to explain the latest data from TJNAF and DESY. Finally, models of hyperon-nucleon and hyperon-hyperon interactions constructed by using SU(3) symmetry were used to investigate the structure of hypernuclei.

“Relativistic effects” in nuclear dynamics depend strongly on definitions and assumptions. We have been concentrating on adjustments of standard Galilei covariant nuclear dynamics required for compliance with covariance under the inhomogeneous Lorentz group (Poincaré group). While covariants transform differently under the two groups, the invariants are effectively identical. We conclude that while it is essential to relate dynamically determined invariants to covariant observables by relativistic kinematics, Poincaré compliance at the 1% level does not require adjustments of standard nuclear Hamiltonians for two and three nucleons. We expect this result to hold for more nucleons as well.

a.1. A Dynamical, Confining Model and Hot Quark Stars (C. D. Roberts, S. Schmidt, D. Blaschke,* H. Grigorian,† and G. Poghosyan‡)

We explored the consequences of an equation of state (EOS) obtained in a confining Dyson-Schwinger equation model of QCD for the structure and stability of non-strange quark stars at finite temperature, T , and compared the results with those obtained using a bag-model EOS. Both models support a temperature profile that varies over the star's volume and the consequences of this are model independent; *e.g.*, the maximum mass of a quark star is reduced as the central temperature is

increased and the maximum attainable radius of a pure quark star is $R \sim 8-10$ km. However, in our model the analogue of the bag pressure is (T, μ) -dependent, which is not the case in the bag model. This is a significant qualitative difference and comparing the results effected a primary goal of elucidating the sensitivity of quark star properties to the form of the EOS. An article describing this work was published.¹

*University of Rostock, Germany, †Yerevan State University, Armenia

¹C. D. Roberts, D. Blaschke, S. Schmidt, H. Grigorian, and G. Poghosyan, Phys. Lett. **B450**, 207 (1999)

a.2. Mean Field Exponents and Small Quark Masses (C. D. Roberts, P. Maris, and A. Höll*)

We demonstrated that the restoration of chiral symmetry at finite-temperature in a class of confining Dyson-Schwinger equation (DSE) models of QCD is a mean field transition, and that an accurate determination of the critical exponents using the chiral and thermal susceptibilities requires very small values of the current-quark mass: $\log_{10}(m/m_{\text{U}}) \sim -5$, making their determination via lattice-QCD simulations very difficult. Other classes of DSE models characterized

by qualitatively different interactions also exhibit a mean field transition. Incipient in this observation is the suggestion that mean field exponents are a result of the gap equation's fermion substructure and not of the interaction. This conclusion can likely only be false if $1/N_c$ -corrections to the quark-gluon vertex are large in the vicinity of the transition. An article describing this work was published.¹

*University of Rostock, Germany

¹C. D. Roberts, P. Maris, and A. Höll, Phys. Rev. C **59**, 1751 (1999)

a.3. Survey of Heavy-meson Observables (C. D. Roberts, M. A. Ivanov,* and Yu. L. Kalinovsky‡)

We employed a Dyson-Schwinger equation model to effect a unified and uniformly accurate description of light- and heavy-meson observables, which we characterized by heavy-meson leptonic decays, semileptonic heavy-to-heavy and heavy-to-light transitions: $B \rightarrow D^*, D, \dots$; $D^0 \rightarrow K^*, K$; radiative and strong decays: $B^* \rightarrow B$; $D^* \rightarrow D, D$; and the rare $B \rightarrow K^*$ flavor-changing neutral-current process. We elucidated the heavy-quark limit of these processes and, using a model-independent mass formula valid for all nonsinglet pseudoscalar mesons, demonstrated that their mass rises linearly with the mass of their heaviest constituent. In our numerical calculations we eschewed

a heavy-quark expansion and relied instead on the observation that the dressed c, b -quark mass functions are well approximated by a constant, interpreted as their constituent-mass: we found $\hat{M}_c = 1.29$ GeV and $\hat{M}_b = 4.54$ GeV. The calculated heavy-meson leptonic decay constants and transition form factors are a necessary element in the experimental determination of CKM matrix elements. The results also show that this framework, as employed hitherto, is well able to describe vector meson polarization observables. An article describing this work was published.¹

*BLTP, JINR, Dubna, †LCTA, JINR, Dubna,

¹C. D. Roberts, M. A. Ivanov, and Yu. L. Kalinovsky, Phys. Rev. D **60**, 34018 (1999)

a.4. Electromagnetic Nucleon Form Factors (J. C. R. Bloch, C. D. Roberts, S. M. Schmidt, A. Bender,* and M. R. Frank†)

We calculated the nucleon's electromagnetic form factors on q^2 [0,3] GeV^2 using an *Ansatz* for the nucleon's Fadde'ev amplitude motivated by quark-diquark solutions of the relativistic Fadde'ev equation. In this first study only the scalar diquark is retained, and it and the quark are confined. A good description of the data requires a nonpointlike diquark correlation with an electromagnetic radius of 0.8 r . The

composite, nonpointlike nature of the diquark is crucial. It provides for diquark-breakup terms that are of greater importance than the diquark photon absorption contribution. This is a first and important step in extending the successful, Dyson-Schwinger-equation-based meson phenomenology to the baryon sector, a long-held goal. An article describing this research was published.¹

*University of Adelaide, Australia, †Institute for Nuclear Theory, Seattle

¹J. C. R. Bloch, C. D. Roberts, S. M. Schmidt, A. Bender, M. R. Frank, Phys. Rev. C **60**, 062201 (Rapid Comm.) (1999)

a.5. Diquarks: Condensation without Bound States (J. C. R. Bloch, C. D. Roberts, and S. M. Schmidt)

We employed a bispinor gap equation to study superfluidity at nonzero chemical potential, $\mu < 0$, in two- and three-color QCD. The two-color theory, QC2D, is an excellent exemplar: the order of truncation of the quark-quark scattering kernel, K , has no qualitative impact, which allows a straightforward elucidation of the effects of μ when the coupling is strong. In rainbow-ladder truncation, diquark bound states appear in the spectrum of the three-color theory, a defect that is eliminated by an improvement of K . The

corrected gap equation describes a superfluid (diquark condensed) phase that is semi-quantitatively similar to that obtained using the rainbow truncation. A model study suggests that the width of the superfluid gap and the transition point in QC2D provide reliable quantitative estimates of those quantities in QCD. The diquark superfluid may exist at the core of dense astrophysical objects. An article describing this research was published.¹

¹J. C. R. Bloch, C. D. Roberts, and S. M. Schmidt, Phys. Rev. C **60**, 065208 (1999)

a.6. Describing a_1 and b_1 Decays (J. C. R. Bloch, C. D. Roberts, S. M. Schmidt, and Yu. L. Kalinovsky*)

Two-body pion-radiating and weak decays of light axial-vector mesons and the D/S ratios were studied as a phenomenological application of the QCD Dyson-Schwinger equations. We found that models based on the rainbow-ladder truncation are capable of providing a good description and, in particular, yield the correct

sign and magnitude of the a_1 and b_1 D/S ratios, with no additional mechanism necessary. The study confirms that this ratio is sensitive to the long-range part of the quark-quark interaction and can be used to constrain model forms. An article describing this research was published.¹

*LCTA, JINR, Dubna

¹J. C. R. Bloch, Yu. L. Kalinovsky, C. D. Roberts, and S. M. Schmidt, Phys. Rev. D **60**, 111502 (Rapid Comm.) (1999)

a.7. Pair Creation: Back-Reactions and Damping (J. C. R. Bloch, C. D. Roberts, S. M. Schmidt, V. A. Mierny,* A. V. Prozorkevich,* S. A. Smolyansky,* and D. M. Vinnik*)

As a step toward understanding the kinetic evolution from a relativistic heavy-ion collision to a quark-gluon plasma we solved the quantum Vlasov equation for fermions and bosons, incorporating spontaneous pair creation in the presence of back-reactions and collisions. Pair creation is initiated by an external impulse field that models an energetic heavy-ion collision and the source term is non-Markovian; *i.e.*, it is non-local in time. A simultaneous solution of Maxwell's equation in the presence of feedback yields

an internal current and electric field that exhibit plasma oscillations with a period τ_{pl} , just as would a plasma in QED. Allowing for collisions, these oscillations are damped on a time-scale, τ_r determined by the collision frequency. We find that plasma oscillations cannot affect the early stages of the formation of a quark-gluon plasma unless $\tau_r \gg \tau_{pl}$ and $\tau_{pl} \sim 1/\omega_{QCD} \sim 1 \text{ fm}/c$. That will make it difficult to observe this effect at RHIC. An article describing this research was published.¹

*Saratov State University, Armenia

¹J. C. R. Bloch, V. A. Mizerny, A. V. Prozorkevich, C. D. Roberts, S. M. Schmidt, S. A. Smolyansky and D. V. Vinnik, Phys. Rev. D **60**, 116011 (Rapid Comm.) (1999)

a.8. K and a Light Scalar Meson (J. C. R. Bloch, C. D. Roberts, S. M. Schmidt, M. A. Ivanov,* and T. Mizutani†)

We explored the $I = 1/2$ rule and the fundamental CP violating gauge: $1/\Lambda$ in K transitions using the Dyson-Schwinger equations. Exploiting the feature that QCD penguin operators direct $\chi_{\pi\pi}$ transitions through 0^{++} intermediate states, we find an explanation of the enhancement of $I = 0$ K transitions in the contribution of a light π -meson, $m_{\pi} \approx 0.5 \text{ GeV}$. This

mechanism also affects $1/\Lambda$ providing a significant enhancement. The study shows that the effect of this π -meson should be understood before any conclusions can be drawn about non-Standard-Model effects in parity violating K-decays. An article describing this work was submitted for publication.

*BLTP, JINR, Dubna, †Virginia Polytechnic Institute and State University, Blacksburg, VA.

a.9. Memory Effects and Thermodynamics in Strong Field Plasmas (J. C. R. Bloch, C. D. Roberts, and S. M. Schmidt)

Continuing our exploration of nonequilibrium aspects of ultrarelativistic heavy-ion collisions, we studied the evolution of a strong-field plasma using a quantum Vlasov equation with a non-Markovian source term and a simple collision term. This provided calculated results for the time-dependence of the energy density and particle-number density. We found that the evolution of a plasma produced with RHIC-like initial conditions is well described by a low-density

approximation to the source term, with non-Markovian effects and plasma oscillations unlikely to be observable. However, with the much larger initial energy density in an LHC-like collision, non-Markovian effects and plasma oscillations certainly influence the evolution of the plasma. These effects may even be observable in the spectrum of dileptons emitted before equilibration of the plasma. An article describing this work was published.¹

¹J. C. R. Bloch, C. D. Roberts, and S. M. Schmidt, Phys. Rev. D **61**, 117502 (2000)

a.10. Selected Nucleon Form Factors and a Composite Scalar Diquark

(J. C. R. Bloch, C. D. Roberts, and S. M. Schmidt)

As an application and test of our quark-plus-scalar-diquark nucleon model, we calculated a wide range of leptonic and nonleptonic nucleon form factors: pseudoscalar, isoscalar- and isovector-vector, axial-vector and scalar. The last yields the nucleon σ -term and on-shell σ -nucleon coupling. The calculated form factors are soft and there is no sign that this is a model-dependent result, and the couplings are generally in good agreement with experiment and other determinations, as is evident in Table V-1. Elements in the dressed-quark-axial-vector vertex that are not constrained by the Ward-Takahashi identity contribute

$\sim 20\%$ to the magnitude of g_A , as the comparison between the results labeled a) *etc.* in the table indicate. We anticipate a contribution of similar magnitude from the axial-vector diquark correlation, hitherto omitted. The calculation of the nucleon σ -term is particularly interesting because it illustrates the only method that allows an unambiguous off-shell extrapolation in the estimation of meson-nucleon form factors. The calculated form factor is depicted in Fig. IV-1. An article describing this work was submitted for publication.

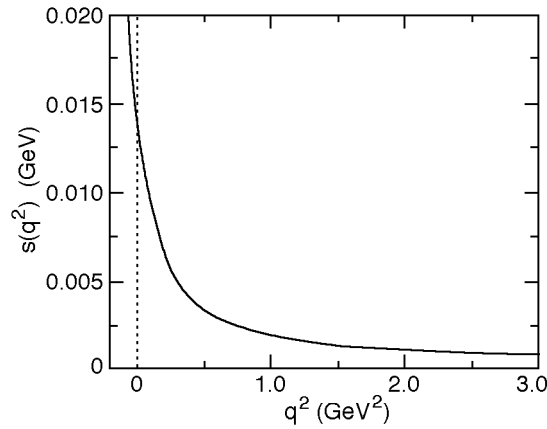


Fig. V-1. Calculated form of $\sigma(q^2)$. The rapid increase with decreasing q^2 is associated with the evolution to the σ -meson pole. A good fit to the result is: $\sigma(t) = g(t) \frac{m_\sigma^2}{1 - t/m_\sigma^2}$ with the renormalization group invariant product

$m_\sigma = 3.3 \text{ MeV}$ and $g(t) = 1.61 + 2.61 \frac{1}{(1 - t/2)^{10}}$ with $m_\sigma = 1.56 \text{ GeV}$. The on-shell sigma-nucleon coupling is $g_{NN} = 27.7$.

Table V-1. Calculated nucleon couplings compared with: contemporary meson exchange model values, where available; experiment in the case of g_A , r_A ; a lattice-QCD result for χ . For the VNN couplings the labels “a)” *etc.* identify the results obtained with different *Ansätze* for the vector meson Bethe-Salpeter amplitude; and for g_A and r_A the label b) indicates the inclusion of the a_1 -meson's contribution to the dressed-quark-axial-vector vertex.

	Calc.	Estimates	Expt.
g_{NN}	14.9	13.4	
$\langle r_{NN}^2 \rangle^{1/2}$	a) 0.71 b) 0.80	0.93 – 1.06 fm	
g_{NN}	a) 5.92 b) 6.26 c) 4.82	6.4	
f_{NN}	a) 15.4 b) 16.6 c) 12.6	13.0	
	a) 2.57 b) 2.64 c) 2.61	2.0	
g_{NN}	a) 9.74 b) 10.2 c) 11.5	7 – 10.5	
f_{NN}	a) 9.62 b) 10.7 c) 4.39		
	a) 0.99 b) 1.04 c) 0.38		
g_A	a) 0.80 b) 0.99		1.259 ± 0.017
$\langle r_A^2 \rangle^{1/2}$	a) 0.75 b) 0.75		0.68 ± 0.12 fm
χ/M_N	0.015	0.019 ± 0.05	
g	9.3	10	
$\langle r^2 \rangle^{1/2}$	0.89	1.2 fm	

a.11. Temperature-Dependence of Pseudoscalar and Scalar Correlations

(C. D. Roberts, S. M. Schmidt, P. Maris,* and P. C. Tandy*)

In order to elucidate hadronic signals of quark-gluon plasma formation we solved the inhomogeneous pseudoscalar and scalar Bethe-Salpeter equations using a renormalization-group-improved rainbow-ladder truncation. The solutions exhibit bound state poles below and above T_c , the critical temperature for chiral symmetry restoration, *i.e.*, the bound states persist into the quark gluon plasma. Above T_c the bound state amplitudes are identical, as are the positions and residues of the pseudoscalar and scalar poles in the vertices, and so these composites are identical in the

absence of dynamical chiral symmetry breaking. We found that in the chiral limit the σ coupling vanishes at T_c , as do f , m and g . Furthermore, for light current-quark masses the ρ decay channel of the isoscalar-scalar meson remains open until very near T_c , and the widths of the dominant pion decay modes remain significant in the vicinity of the crossover. Therefore one cannot expect to identify the quark gluon plasma via a marked increase in the ρ -meson lifetime. An article describing this research was submitted for publication.

*Kent State University

a.12. Axial-Vector Diquarks in the Baryon

(C. D. Roberts, S. M. Schmidt, and M. B. Hecht)

We have seen that a product *Ansatz* for the nucleon's Faddeev amplitude using only a scalar-diquark provides a very good description of leptonic and nonleptonic couplings and form factors, with some notable exceptions, *e.g.*, r_n^2 and g_A . We anticipate that the inclusion of axial-vector diquark correlations will significantly improve the description in these exceptional cases. Furthermore, without axial-vector

diquark correlations we can't describe the Δ resonance, or the N transition, which is an important probe of hadron structure and models. For example, resonant quadrupole strength in this transition can be interpreted as a signal of nucleon deformation. Hence we are currently working on improving the *Ansatz* by including these qualitatively important correlations.

a.13. J/ψ Suppression as a Signal of Quark-Gluon Plasma Formation

(C. D. Roberts, S. M. Schmidt, M. B. Hecht, and D. B. Blaschke*)

We have developed a successful approach to describing heavy-meson observables at zero temperature. That makes possible a reliable extrapolation into the domain of nonzero temperature, which is relevant to the program at RHIC. The suppression of the J/ψ production cross section has been touted as a unique signal for quark-gluon plasma formation, and such a suppression has been observed at CERN. We are studying J/ψ production in the expectation that

additional insight will follow from the Dyson-Schwinger equations' unique capacity to unify nonperturbative aspects of light- and heavy-meson observables via a microscopic description using QCD's elementary excitations. Our goal is to elucidate the mechanisms involved and the fidelity of J/ψ suppression as a signal of quark gluon plasma formation.

*University of Rostock, Germany

a.14. Pre-equilibrium Signals of Plasma Formation (C. D. Roberts, S. M. Schmidt, and M. B. Hecht)

Nonequilibrium aspects of quark-gluon plasma formation remain an important focus and we aim to connect such pre-equilibrium effects as plasma oscillations and non-Markovian features of the source term with observable signals in the dilepton spectrum. A further improvement is to include a realistic description of quark propagation in the deconfined domain. Although chiral symmetry is restored, as

evident in a marked suppression of the scalar piece of the dressed-quark's self energy, nonperturbative effects persist in the vector piece of the self energy. These have important, observable consequences in equilibrium, such as a softening of the equation of state, and may also quantitatively affect the pre-equilibrium phase.

a.15. Dynamical Test of Constituent Quark Models with N Reactions (T.-S. H Lee, T. Yoshimoto,* T. Sato,* and M. Arima†)

A dynamical approach is developed to predict the N scattering amplitudes starting with the constituent quark models. The first step is to apply a variational method to solve the three-quark bound state problem. The resulting wave functions are used to calculate the N^*

N , N , vertex functions by assuming that the N and mesons couple directly to quarks. These vertex functions and the predicted baryon bare masses then define a Hamiltonian for N reactions. We apply a unitary transformation method to derive from the constructed Hamiltonian a multi-channel and multi-resonance reaction model for predicting the N scattering amplitudes up to $W = 2$ GeV. With the

parameters constrained by the (1232) excitation, we have shown that the N scattering in S_{11} channel cannot be described by constituent quark models based on the one-gluon-exchange (OGE) or one-meson-exchange (OME) mechanisms. Our results are shown in Fig. V-2. It is found that the data seem to favor the spin-spin interaction due to one-meson-exchange and the tensor interaction due to one-gluon-exchange. A phenomenological quark-quark potential has been constructed to reproduce the S_{11} amplitude. A paper describing our results has been submitted to Physics Review C.

*Osaka University, Japan., †Osaka City University, Japan

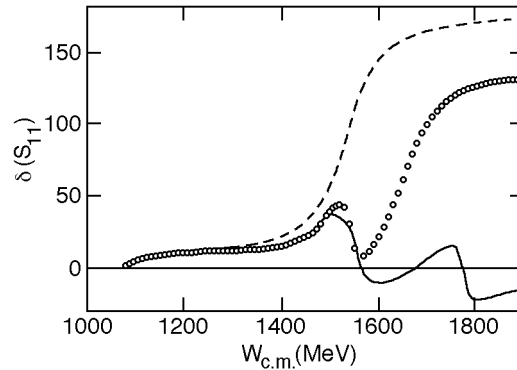


Fig. V-2. Phase shifts of N scattering in the S_{11} channel. The solid and dashed curves are results from the OGE and OME models, respectively. Open circles are the data.

a.16. Determination of the N- Form Factors with $p(e, e^0)$ Reactions
(T.-S. H. Lee and T. Sato*)

The Hamiltonian model developed in Ref. 1 has been extended to investigate pion electroproduction on the nucleon. Guided by the results obtained from our previous study¹ of pion photoproduction, we assume that the strengths $G_M(0)$, $G_E(0)$, $G_C(0)$ of the bare N vertex can be related to each other within the constituent quark model. For $G_M(0) = 1.85(1.95)$, $G_E(0) = 0.025(-0.025)$ determined in Ref. 1, we obtain $G_C(0) = -0.2241(0.2195)$. The only freedom in our calculations is the Q^2 -dependence of the N- form factors. In a first attempt, we have found that all of the available $p(e, e^0)$ data can be described to a

very large extent if we assume that the bare N- form factor has the Q^2 -dependence $F_N(Q^2) = [1 + Q^2/4M_{ave}^2]^{1/2} [1 + Q^2/4]^{-1} G_E^p(Q^2)$, where $M_{ave} = (m_N + m) / 2G_E^p(Q^2)$ is the usual proton electric form factor and $= 1.2$ GeV. Some sample results are compared in Fig. V-3 with the recent data² at $Q^2 = 2.78$ (GeV/c)² from Jefferson Laboratory. More detailed results will be presented to give a more sophisticated quark model interpretation of the determined bare N- form factors.

*Osaka University, Japan

¹T. Sato and T.-S. H. Lee, Phys. Rev. C **54**, 2660 (1996)

²V. V. Frolov, *et. al.*, Phys. Rev. Lett. **82**, 45 (1998)

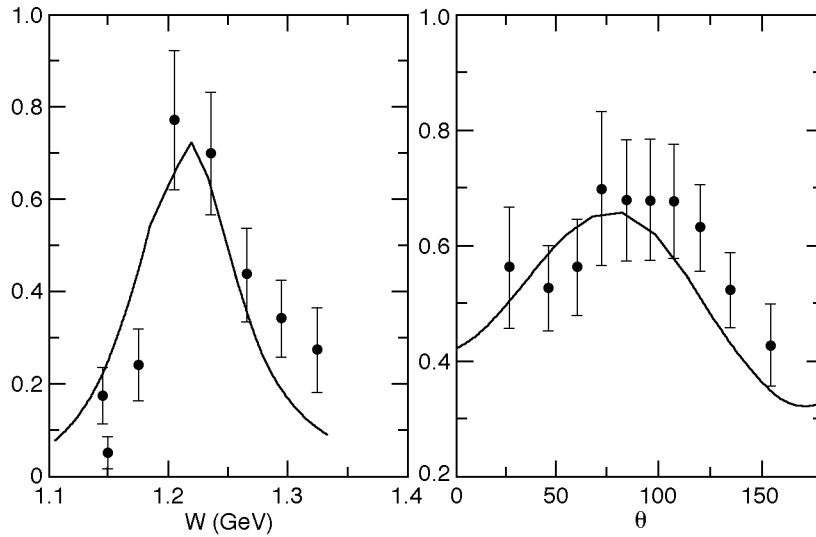


Fig. V-3. Differential cross section of $p(e, e^0)$ at $Q^2 = 2.78$ (GeV/c)².

a.17. Structure of the Vector Meson Photoproduction Amplitude at a Few GeV

(T.-S. H. Lee, A. I. Titov*, and H. Toki†)

The structure of the photoproduction amplitude in the $s \sim 2\text{-}5$ GeV region is analyzed based on Pomeron-exchange and meson-exchange mechanisms. The SU(3) symmetry and the decay widths are exploited to determine the parameters that are needed to predict the amplitudes due to pseudoscalar meson (π^0, η) exchange, scalar meson (σ, a_0, f_0) exchange, and the ω -radiation from the nucleon. In addition to the universally accepted Pomeron exchange with an intercept $\alpha(0) \sim 1.08$, we investigate the role of a second Pomeron with $\alpha(0) < 0$, as inspired by the glueball ($J = 0^+, M_b^2 \sim 3 \text{ GeV}^2$) predicted by Lattice QCD calculations and the Dual Landau-Ginsburg

model. It is found that the existing limited data at low energies near threshold can accommodate either the second Pomeron or the scalar meson exchange. The differences between these two competing mechanisms are shown to have profound effects on various density matrices which can be used to calculate the cross sections as well as various single- and double-polarization observables. We predict a definite isotopic effect: polarization observables of photoproduction on the proton and neutron targets can have differences of a factor 2 and more. Two papers describing our results have been published^{1,2}.

*JINR, Dubna, Russia, †Osaka University, Japan

¹A. I. Titov, T.-S. H. Lee, H. Toki, and O. Streltsov, Phys. Rev. C **60**, 035205 (1999)

²A. I. Titov, T.-S. H. Lee, and H. Toki, Phys. Rev. C **59**, R2993 (1999)

a.18. Evidence for the Fourth P_{11} Resonance Predicted by the Constituent Quark Model

(T.-S. H. Lee, Simon Capstick,* W. Roberts,† A. Svarc‡)

It is pointed out that the third of five low-lying P_{11} states predicted by a constituent quark model can be identified with the third of four states in a solution from a three-channel analysis of N scattering amplitudes. This is one of the so-called “missing” resonances,

predicted at 1880 MeV. The fit to the $N \rightarrow N$ data is the crucial element in finding this fourth resonance in the P_{11} partial wave. A paper describing our results has been published¹.

*Florida State University, †National Science Foundation, ‡Rudjer Boskovic Institute, Croatia.

¹T.-S. H. Lee, Simon Capstick, W. Roberts and A. Svarc, Phys. Rev. C **59**, R3002 (1999)

a.19. Strange Hadron Matter and SU(3) Symmetry (T.-S. H. Lee and V. G. J. Stoks*)

We calculate saturation curves for strange hadron matter using the SU(3) baryon-baryon potentials of Ref. 1. All possible interaction channels within the baryon octet (consisting of N, Σ, Λ) are considered. It is found that a small fraction in nuclear matter slightly increases binding, but that larger fractions ($>10\%$) rapidly cause a decrease. Charge-neutral N, Σ, Λ systems, with equal densities for nucleons and

hyperons, are only very weakly bound. The dependence of the binding energies on the strangeness per baryon, f_S , is predicted for various N, Σ, Λ and $N, \Sigma, \Lambda, \Xi, \Omega$ systems. The implications of our results in relativistic heavy-ion collisions and the core of a dense star are discussed. We also discuss the differences between our results and previous hadron matter calculations. A paper describing our results has been published².

*University of Adelaide, Australia

¹V. G. J. Stoks and Th. A. Rijken, Phys. Rev. C **59**, 21 (1999)

²V. G. J. Stoks and T.-S. H. Lee, Phys. Rev. C **60**, 024006 (1999)

a.20. Study of Hyperon-Nucleon Interactions with $d(e,e'K)$ Reactions

(T.-S. H. Lee, P. Oswald,* and B. Saghai*)

The $d(e,e'K^+)$ reaction has been investigated by using the kaon production amplitudes developed by the Saclay-Lyon collaboration. Our focus is on the dependence of the reaction cross sections on the final hyperon-nucleon interactions, aiming at testing the

SU(3) models of baryon-baryon potentials. To fix the $N \rightarrow \Lambda$ KY amplitude, we are refining the Saclay-Lyon amplitudes to fit the new data from TJNAF and extending the model to also account for kaon production on the neutron.

*CEA-Saclay, France

a.21. Particle-Hole Folded-Diagram Calculation of the Hypernucleus ${}^{16}_{\Lambda}\text{O}$ Using

Meson-Exchange Interactions (T.-S. H. Lee, Yiharn Tzeng,* S. Y. Tsay Tzeng,† and T. S. Kuo‡)

The ${}^{16}_{\Lambda}\text{O}$ hypernucleus is investigated by way of a folded-diagram method. The input G-matrix elements are calculated accurately from the Jülich- \bar{B} and the Nijmegen realistic hyperon-nucleon potentials with the Pauli exclusion operator properly treated in the finite hypernuclear system. The effect of hyperon-nucleon-nucleon three-body forces is included through the consideration of core polarization diagrams. Although our predicted energy spectrum of the hypernucleus is in good agreement with experiments in general, there are

significant differences between the positive parity energy levels obtained from these two realistic potentials. A folded-diagram calculation for the single-particle energy has been performed. The spin-dependence parameters of Millener *et al.* calculated from the Jülich- \bar{B} and Nijmegen potentials are significantly different from each other, and the contribution from the Λ - Λ three-body force to these parameters is important. A paper describing our results has been published¹.

*Academia Sinica, Taiwan, †National Taipei University of Technology, Taiwan, ‡SUNY, Stony Brook

¹T.-S. H. Lee, Yiharn Tzeng, S. Y. Tsay Tzeng, and T. T. S. Kuo, Phys. Rev. C **60**, 044305 (1999)

a.22. Two-frequency Shell Model for Hypernuclei (T.-S. H. Lee, T. T. S. Kuo,* and

Y. Tzeng†)

A two-frequency shell model is proposed for investigating the structure of hypernuclei starting with a hyperon-nucleon potential in free space. In a calculation for ${}^{16}_{\Lambda}\text{O}$ using the folded-diagram method, the applicability of the model is demonstrated by showing that the predicted single-particle energies have saturation minima at an oscillator frequency $\hbar \omega \sim 10$ MeV, which is considerably smaller than $\hbar \omega_{N=14}$

MeV for the nucleon orbits. A fairly strong dependence on $\hbar \omega$ has also been observed for the calculated particle-nucleon hole interactions. The model has been applied to demonstrate that the Λ - Λ NN three-body force induced by the $N \leftrightarrow \Lambda$ transitions can significantly change the predicted spectrum. A paper describing our results has been published¹.

*SUNY at Stonybrook, †Academia Sinica, Taiwan

¹T.-S. H. Lee, T. T. S. Kuo, and Y. Tzeng, Phys. Rev. C **61**, 031305 (2000)

a.23. Effect of Neutron Excess on Excitations in Exotic Nuclei (T.-S. H. Lee, Mahmoud A. Hasan,* and James P. Vary†)

The effects of neutron excess on the formation of $(3,3)$ resonance states in exotic nuclei at equilibrium and under large amplitude compression have been investigated within the radial constraint spherical Hartree-Fock method. An effective Hamiltonian has been used which includes the degree of freedom explicitly. Results are presented for ^{28}O , ^{60}Ca , and ^{70}Ca in a model space of seven major oscillator shells and eight orbitals. The results show that the formation of the $(3,3)$ depends strongly on the amount of neutron excess in the nuclear system. In contrast to previous work where we found no $(3,3)$ in ^{16}O and ^{40}Ca

at equilibrium, these results show that a significant amount of $(3,3)$ exists at equilibrium in exotic isotopes. In addition, as the nucleus is compressed to a density of 2.5 times the ordinary nuclear density, the percentage of the $(3,3)$ rises to 3%, 5%, and 7% of the total number of all baryons in ^{28}O , ^{60}Ca , and ^{70}Ca , respectively. This suggests a parameterization for the percentage of the $(3,3)$ created at 2.5 times the normal density of the form $0.25(N-Z)\%$. The results are consistent with the theoretical prediction of the formation of $(3,3)$ matter in neutron-rich matter at high compression. A paper describing our results has been published¹.

*Applied Science University, Jordan, †Iowa State University, Ames

¹T.-S. H. Lee, Mahmoud A. Hasan, and James P. Vary, Phys. Rev. C **61**, 014301-1 (2000)

a.24. Quantum Monte Carlo Calculations of Pion Inelastic Scattering from Li (T.-S. H. Lee and R. B. Wiringa)

Quantum Monte Carlo methods have been successfully developed to predict the properties of low-lying states of light nuclei starting with realistic two- and three-nucleon potentials. The predicted proton transition densities were found to be in good agreement with the (e,e') data both in shape and absolute magnitude. By carrying out the Distorted-Wave-Impulse-Approximation calculations of pion inelastic scattering from Li in the $(3,3)$ region, we have found that the

predicted neutron excitations are also in good agreement with the data. The large enhancement factors (about 2) for quadrupole excitations within the conventional shell-model are not needed in this calculation. This has resolved one of the long-standing structure problems encountered in the studies of pion-nucleus reactions. Our results are compared with the data in Fig. V-4 for ^7Li . Calculations for Be are now in progress.

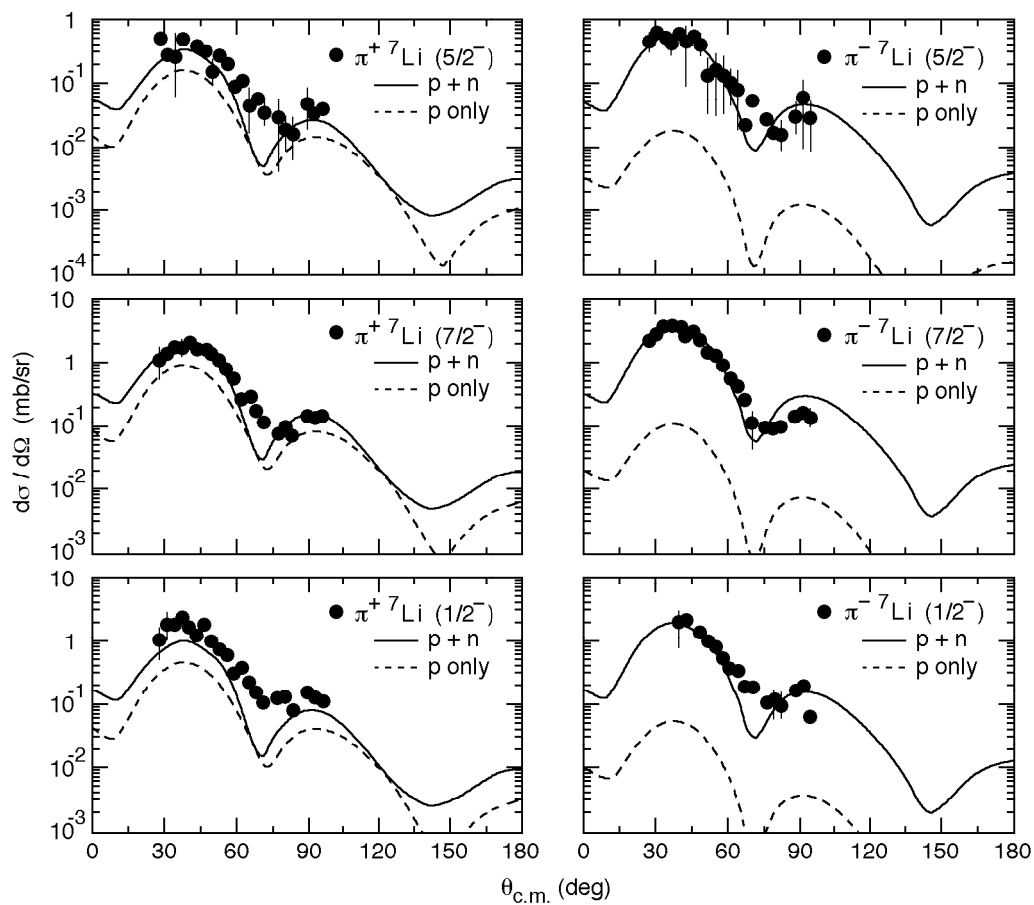


Fig. V-4. The differential cross section for ${}^7\text{Li}(\pi, \pi')$.

a.25. On “Ambiguities” of Spin-1 Form Factors in Null-Plane Dynamics (F. Coester)

It is an inescapable feature of relativistic Hamiltonian dynamics that single-particle current density operators are covariant only under the kinematic subgroup. In practice the interaction dependence of fully covariant current matrices is obtained by transforming a subset of single-particle current matrix elements with the dynamic Poincaré representations. This process invariably involves physically motivated choices, specifically the choice of the kinematically-invariant hypersurface in relation to relevant four-vectors of the system. With null-plane dynamics the kinematic subgroup is determined by a null-vector, which for spin-1 systems can be related to three mutually orthogonal four-vectors: the four-momentum transfer Q , the projection \tilde{P} of the four-momentum operator orthogonal to Q , and the transverse polarization four-vector S . In most applications the null-vector has been chosen orthogonal to Q . This choice has the virtue that $Q^2 = Q^2$ is a kinematic quantity

independent of the masses. Subject to this constraint the null-vector can be any linear combination of \tilde{P} , S , and the unit vector perpendicular to both, as well as to Q . Different authors have used different prescriptions corresponding to different angles between the null-vector and S .¹ The matrix elements that determine the form factors also involve the longitudinal polarization vectors S_{\parallel} and S'_{\parallel} that are orthogonal to the initial and final four-momenta respectively. Only when the null-vector is perpendicular to the transverse polarization vector can the longitudinal polarization vectors be independent of the initial and final masses. This choice has the unique advantage that the current construction is equally applicable to inelastic transitions. The prescription resulting in this way is identical to that obtained by Karmanov treating the orientation of the null vector as an unphysical degree of freedom.^{2,3}

¹V.A. Karmanov, Nucl. Phys A **608**, 316 (1996)

²J. Carbonell *et al.*, Physics Reports **360**, 216 (1998)

³F. Coester, W. H. Klink, and W. N. Polyzou Few Body Systems Supp. **10**, 115 (1999)

a.26. Poincaré Compliance of Standard Nuclear Dynamics¹ (F. Coester, W. H. Klink,* and W. N. Polyzou*)

Standard Hamiltonian nuclear dynamics¹ is a mathematically consistent framework for the quantitative description of nuclei. The form of the two-nucleon Hamiltonian is suggested by quantum field theory while the quantitative details are adjusted to fit a vast array of available two-nucleon data. Much smaller three-body forces are similarly determined. Assuming that higher-order multi-nucleon forces are negligible the Hamiltonian is then completely determined for any nucleon number. Conserved electromagnetic currents consistent with these nuclear forces are available.² Detailed numerical work has produced remarkable agreement with many data. Calculations of binding energies and energy levels of light nuclei are accurate

to about 1% so that larger discrepancies with data can be attributed to an inadequacy of the Hamiltonian.

There is a possible objection of principle in that the standard nuclear dynamics does not respect the fundamental space time symmetry of the inhomogeneous Lorentz group (Poincaré group).³ Crude estimates of “relativistic effects” suggest that they might be as large as 10%. In this context it is important to separate requirements suggested by features of relativistic quantum field theory from the space-time symmetry requirements. Standard nuclear dynamics is Galilei covariant. The question addressed here is what modification of the dynamics is required

*University of Iowa

¹F. Coester, Symposium on Current Topics in the Field of Light Nuclei, Cracow, (1999) p. 1000

²J. Carlson and R. Schiavilla, Rev. Mod. Phys. **70**, 743 (1009)

³S. Weinberg, Quantum Theory of Fields, Vol. **1**, Chapter 2

⁴F. Coester, Helv. Phys. Acta **38**, 7 (1965)

⁵B. D. Keister and W. N. Polyzou, Advances in Nuclear Physics, Vol. **20** p. 225 Sec. 3 (1991)

to achieve ‘‘Poincaré compliance’’, that is Poincaré covariance and cluster separability of the observables.⁴ The answer depends on a comparison of the relevant irreducible unitary (projective) representations of the two groups.^{3,5} For both groups the little group is SU(2). The Casimir operators of both groups are the square of the spin and the Casimir Hamiltonians related to the mass (rest energy) of the system. The Poincaré-Casimir Hamiltonian h of an A -nucleon system can be defined as a function of the mass operator M and the nucleon mass m by $h := (M^2 - A^2 m^2)/2Am$. The operator h so defined has the same continuous spectrum including degeneracies as the Galilean Casimir Hamiltonian $h_{NR} := H - \vec{P}^2/2Am$. Thresholds and the point spectra (binding energies) differ by less than 1%. While covariants transform differently under the two groups the invariants are effectively identical. Dynamically-determined wave functions are not observable. Covariant observables, S-matrix elements

and matrix elements of currents, are related to the invariants kinematically.

The realization of S-matrix cluster separability for more than 2 nucleons involve the Clebsch-Gordan and Racah coefficients, which differ for the two groups. For three nucleons it follows from properties of the Galilei and Poincaré Clebsch-Gordan coefficients that no adjustment of standard nuclear Hamiltonians is required to achieve Poincaré compliance. We expect that the required multi-nucleon forces for larger systems will be negligible.

We conclude that while it is essential to relate dynamically determined invariants to covariant observables by relativistic kinematics, Poincaré compliance at the 1% level does not require adjustments of standard nuclear Hamiltonians for two and three nucleons. We expect this result to hold for more nucleons as well.

B. NUCLEAR FORCES AND NUCLEAR SYSTEMS

The goal of this program is to achieve a description of nuclear systems ranging in size from the deuteron and triton to nuclear matter and neutron stars using a single parameterization of the nuclear forces. Aspects of our program include both the construction of two- and three-nucleon potentials and the development of many-body techniques for computing nuclear properties with these interactions. Detailed quantitative, computationally-intensive studies are essential parts of this program.

Quantum Monte Carlo (QMC) calculations of light ($A \leq 9$) nuclei with realistic interactions have been the main focus of our recent efforts. Our nonrelativistic Hamiltonian contains the accurate Argonne v18 two-nucleon (NN) potential, which includes charge-independence-breaking terms, and either the venerable Urbana IX three-nucleon (3N) potential, or one of several new Illinois 3N models. The QMC calculations include both variational (VMC) and Green's function (GFMC) methods. We begin with the construction of variational trial functions based on sums of single-particle determinants with the correct total $J T$ quantum numbers, and then act on them with products of two- and three-body correlation operators. Energy expectation values are evaluated with Metropolis Monte Carlo integration and parameters in the trial functions are varied to minimize the energy. These optimized variational wave functions then can be used to study other nuclear properties. They also serve as a starting point for the GFMC calculations, which systematically remove higher excited-state components from the trial wave functions by a propagation in imaginary time.

We are currently studying all $A \leq 9$ nuclei with experimentally known bound state or resonance energies, including some 50 (25) excited states in VMC (GFMC). These are the first and only calculations treating $A \leq 6$ nuclei directly with realistic NN and 3N interactions. In GFMC calculations, with the new Illinois 3N models, we can reproduce most of the experimental ground- and excited-state energies within 0.5 MeV. The VMC calculations, including two-body charge and current operators, are being used to study weak decays of $A=6-8$ nuclei and for various $(e,e'p)$ and $(e,e'n)$ reactions. They are also being used to obtain astrophysically

interesting cross sections, starting with the reaction ${}^4\text{He}(d, \gamma){}^6\text{Li}$. Finally, we are also studying the properties of neutron drops with the goal of providing additional constraints for the construction of Skyrme interactions that are used in the modeling of neutron-rich nuclei in neutron star crusts.

Studies of hypernuclei are also continuing. This year, we made major revisions to our calculations of single-particle energies in matter, including density-dependent effective N and NN interactions. We also continue to examine the effect of Λ -induced distortion of nuclear cores in light hypernuclei.

b.1. Variational Monte Carlo Calculations of Light p-shell Nuclei (R. B. Wiringa, S. C. Pieper, K. Varga, V. R. Pandharipande,* and J. Carlson†)

We have completed a major study of $A = 8$ nuclei, and initiated the first calculations for $A = 9$ nuclei. These calculations use the realistic Argonne v_{18} two-nucleon and Urbana IX three-nucleon potentials. The variational wave functions, $\psi(\mathbf{R})$, obtained in these calculations are used as input to the more precise Green's function Monte Carlo (GFMC) calculations described below, and are also being used to study electron scattering and low-energy electroweak reactions of these nuclei. A major paper on the $A = 8$ calculations was recently accepted for publication.¹

Construction of the variational trial function starts with a Jastrow core that includes single-particle orbitals LS-coupled to the desired JM values, as well as pair and triplet spatial correlations. This Jastrow core is then acted on by products of two-body spin, isospin, tensor, and spin-orbit correlation operators and three-body correlation operators for the $3N$ interaction. The wave functions are diagonalized in the small basis of different Jastrow spatial symmetry components to project out higher excited states with the same quantum numbers as the ground or first excited states.

To date we have made calculations for the ground states of all the $A = 6-9$ nuclei, and for 50 different excited states (not counting isobaric analogs); some

recent results are shown in Table IV-2. The binding energies of the ground states are 3–10 MeV high compared to the final GFMC results. However, the excited state energies are in generally good agreement with those GFMC excitations (compared to their respective ground states) that have been calculated. Compared to experiment, these states generally occur in the correct order and with reasonable excitation energies. We have also computed all the isobaric analog multiplets to extract the isovector and isotensor energy differences, and we have calculated the isospin-mixing matrix elements in ${}^8\text{Be}$ excited states.

Current efforts focus on the search for low-lying even-parity intruder states in the $A = 9$ nuclei, and on the construction of improved variational wave functions that build in cluster substructure and have better asymptotic properties. For example, the present ${}^8\text{B}$ wave function treats all four p-shell nucleons equally, but there should be an asymptotic ${}^7\text{Be} + p$ behavior, with ${}^7\text{Be}$ itself having a significant $+$ cluster substructure. This behavior will be important in determining aspects of the proton halo, and in studying important reactions of astrophysical interest. Similar considerations will be even more important in the $A = 9, 10$ nuclei.

*University of Illinois at Urbana-Champaign, †Los Alamos National Laboratory.

¹R. B. Wiringa, S. C. Pieper, J. Carlson, and V. R. Pandharipande, Phys. Rev. C, to be published.

Table V-2. VMC and GFMC excitation energies (in MeV) computed with the Argonne v18 + Urbana IX interaction compared to the experimental spectrum for $A = 8$ nuclei.

${}^A_Z(J^\pi; T)$	VMC	GFMC	Experiment
${}^8\text{He}(2^+; 2)$	2.22(16)	3.01(23)	3.59
${}^8\text{He}(1^+; 2)$	3.32(17)	4.42(25)	
${}^8\text{He}(2^+; 2)$	4.72(18)		
${}^8\text{He}(0^+; 2)$	5.01(17)		
${}^8\text{Li}(1^+; 1)$	1.34(18)	1.03(27)	0.98
${}^8\text{Li}(0^+; 1)$	2.83(19)	1.82(29)	
${}^8\text{Li}(3^+; 1)$	3.35(18)	3.19(28)	2.26
${}^8\text{Li}(2^+; 1)$	3.86(18)		
${}^8\text{Li}(1^+; 1)$	4.22(19)		3.21
${}^8\text{Li}(1^+; 1)$	5.32(19)		5.4
${}^8\text{Li}(4^+; 1)$	6.08(18)	6.88(27)	6.53
${}^8\text{Li}(2^+; 1)$	6.20(18)		
${}^8\text{Li}(3^+; 1)$	7.31(18)		
${}^8\text{Li}(0^+; 2)$	11.24(18)	12.10(25)	10.82
${}^8\text{Be}(2^+; 0)$	2.39(25)	2.91(25)	3.04
${}^8\text{Be}(4^+; 0)$	9.95(24)	9.58(27)	11.4
${}^8\text{Be}(2^+; 1)$	18.60(23)	18.02(27)	16.63*
${}^8\text{Be}(2^+; 0)$	20.29(24)		16.92*
${}^8\text{Be}(1^+; 1)$	19.89(23)		17.64
${}^8\text{Be}(1^+; 0)$	20.03(23)	18.09(33)	18.15
${}^8\text{Be}(1^+; 0)$	21.73(24)		
${}^8\text{Be}(3^+; 1)$	21.77(22)		19.07
${}^8\text{Be}(3^+; 0)$	21.85(24)	19.53(33)	19.24
${}^8\text{Be}(4^+; 0)$	25.85(22)		19.86
${}^8\text{Be}(2^+; 0)$	23.61(23)		20.1
${}^8\text{Be}(3^+; 0)$	25.53(23)		
${}^8\text{Be}(0^+; 0)$	28.62(26)		20.2
${}^8\text{Be}(0^+; 2)$	29.55(22)	29.93(25)	27.49

b.2. Green's Function Monte Carlo Calculations of Light p-shell Nuclei

(S. C. Pieper, R. Roncaglia, R. B. Wiringa, J. Carlson,* and V. R. Pandharipande†)

In the 1980's, the ground states of ${}^2\text{H}$, ${}^3\text{H}$, ${}^3\text{He}$, and ${}^4\text{He}$, and the low-energy scattering states of ${}^5\text{He}$ were studied with Hamiltonians of the form described in the previous section in an essentially exact fashion (limited only by statistical errors) by using the Green's function Monte Carlo (GFMC) method. Our work in the last few years has focused on extending these calculations to light p-shell nuclei and their excited states. These are the first calculations of the structure of such nuclei with realistic many-nucleon Hamiltonians and thus they also test the range of applicability of such Hamiltonians.

In the GFMC calculations, we operate on a trial wave function with the imaginary time propagator, $\exp[-(H'-E_0)\tau]$, where H' is a simplified Hamiltonian, E_0 is an estimate of the eigenvalue, and τ is the imaginary time. To save computer time, the trial wave function is a simplified form of the variational wave functions described in the previous section. The excited-state components of the trial wave function will then be damped out for large τ , leaving the exact lowest eigenfunction with the quantum numbers of the input variational wave function. The expectation value of H is computed for a sequence of increasing values of τ to determine the convergence. Our H' contains the reprojected v_g part of the NN potential and full 3N potential. The small correction $H-H'$ is computed perturbatively. The many-body propagator is written as a symmetrized product of exact two-body propagators, with the 3N potential treated in lowest order.

GFMC calculations for fermion systems suffer from the well-known sign problem in which the statistical error grows exponentially with imaginary time; in our original calculations, this effectively limited τ to 0.06 MeV^{-1} , which means that components of the trial wave function with excitation energies less than $\sim 10 \text{ MeV}$ were not appreciably damped out. In the last two years, we have solved this problem for nuclei by using

"constrained path propagation". In this approach, configurations whose overlap with the trial wave function is small or negative are discarded with a probability such that the average overlap for the discarded configurations is zero. This procedure may not result in an upper bound, but for the very few cases in which it introduces a significant error, a few unconstrained steps result in reliable expectation values. With this method there is no sign problem and we can propagate to arbitrarily large τ . This year we have also realized that a symmetry of the even- A nuclei allows us to save almost 50 percent of the computer time in these cases.

The computer resources (both CPU time and memory) required by our present GFMC method increase exponentially with the number of nucleons. At present calculations of up to $A=8$ nuclei can be routinely made with propagation to $\tau = .2 \text{ MeV}^{-1}$ and we are beginning to explore $A = 9$; in the next few years we might be able to reach $A=12$. However using the present method for larger nuclei will not be practical. To overcome this limit we started work on a cluster-expansion GFMC method. This method, and the computer program, is based on our cluster VMC calculation of ${}^{16}\text{O}$ that was made a few years ago. In the cluster VMC, expectation values are expanded in terms corresponding to the number of nucleons whose spin and isospin degrees of freedom are active. The complete Jastrow wave function is used in every order of the expansion and thus all integrations are $3A$ -dimensional. To extend the method to GFMC, one writes the GFMC mixed estimate for a given τ as an $N \times 3A$ dimensional integral where N is the number of time slices used to reach τ , and then makes the spin- and isospin-cluster expansion of this entire expectation value. Preliminary results obtained for ${}^{16}\text{O}$ and the Argonne v_g' potential using four-body clusters contained large statistical fluctuations. Alternate Monte Carlo sampling methods were tried with inconclusive results.

*Los Alamos National Laboratory; †University of Illinois, Urbana

b.3. Studies of Three-Nucleon Interactions in Nuclear Systems (S. C. Pieper, R. B. Wiringa, V. R. Pandharipande*, D. G. Ravenhall,* and J. Carlson†)

We have made GFMC calculations of the energies of 25 states for nuclei with $3 \leq A \leq 8$ using the Hamiltonian consisting of the Argonne v_{18} NN and Urbana IX 3N potentials. These calculations have shown that this Hamiltonian underbinds p-shell nuclei by 0.8 MeV in ${}^6\text{Li}$ to 5 MeV in ${}^8\text{He}$. The error increases with both A and $|N-Z|$. However, with the exception of some underpredicting of the spin-orbit splittings, the excitation spectra of the nuclei are reasonably well reproduced. The rms error for the 10 ground states is 2.3 MeV and for the 15 excitation energies is 0.5 MeV; with no 3N potential at all these numbers are 7.3 and 0.5 MeV, respectively.

These results show that the simple Urbana 3N potentials, which have been used successfully for more than a decade in studies of s-shell nuclei and dense matter, need to be extended for work in the p-shell. In the last few years, we have been constructing improved "Illinois" models for the 3N potential. Our approach is to use theoretical guidance to suggest the structure of new terms, but to consider the coupling constants and short-range shapes of the potential to be adjustable. This is in the same spirit as the development of realistic NN potentials. We have considered a number of new terms. We find that new potential terms are often not perturbative, *i.e.*, an expectation value of the new term using the GFMC wave function from just Argonne v_{18} and Urbana IX may be misleading. Thus each new term must be added to the GFMC propagator and a new GFMC calculation made. Furthermore, as the strength

of the new term is adjusted, the propagations must be repeated.

The dominant term of the Urbana potential is the Fujita-Miyazawa (FM) two-pion term with intermediate excitation of one nucleon to a Δ . We have now studied three-pion ring terms containing one and two excitations. These are repulsive in s-shell nuclei and attractive in p-shell nuclei and correct the overall loss of binding energy with respect to both A and $|N-Z|$. The Tucson-Melbourne potential contains the FM term and a term arising from s-wave N scattering; we have also considered a corrected s-wave term.

The FM terms in the Urbana 3N potentials and the new models that we first constructed have coupling constants that are about 1/2 the value suggested by soft pion physics. We have also made a model that has the stronger coupling constant; this required a significantly softer cutoff parameter (normally we use the same cutoff as is used in the NN potential). We find that we can obtain excellent fits to the $3 \leq A \leq 8$ binding energies with either class of 3N potential – the rms errors are ~ 500 keV. However the strong coupling constant seems to result in a pion-condensed phase of nuclear matter at much too low a density. We are continuing to investigate this. Figure V-5 compares GFMC values of ground and excited state energies for Urbana IX and one of the new Illinois models to experimental values.

*University of Illinois, Urbana, †Los Alamos National Laboratory

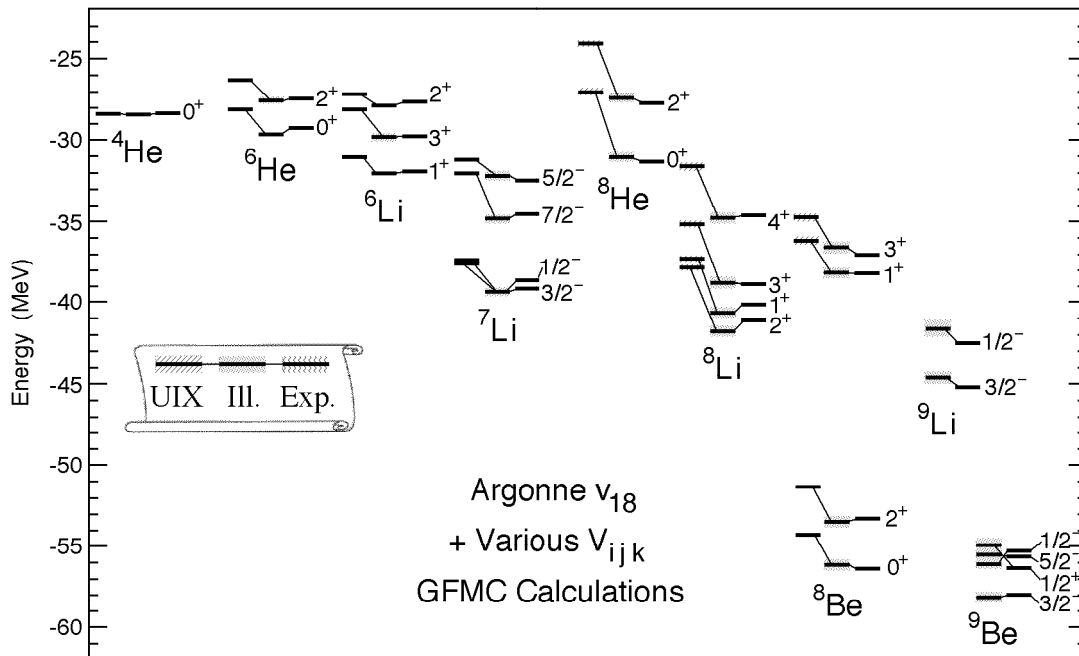


Fig. V-5. Gfmc energies for $A=4-9$ nuclei using the Argonne v_{18} NN potential with either the Urbana IX or one of several new Illinois 3N potentials, compared to experiment.

b.4. Nuclear Structure Studies with (e,e'p) and (e,e'n) Reactions (R. B. Wiringa, L. Lapikás*, and J. Wesseling*)

In previous years we have calculated single-nucleon momentum distributions in many of the $A \leq 8$ nuclei and a variety of cluster-cluster overlap wave functions, such as $dp|{}^3\text{He}$, $dd|{}^4\text{He}$, and $d|{}^6\text{Li}$. More recently we have begun studying overlaps such as ${}^6\text{He} + p|{}^7\text{Li}$ and ${}^6\text{Li} + n|{}^7\text{Li}$. These overlaps can be used to predict the results of exclusive (e,e'p) and (e,e'n) measurements and various pickup or stripping reactions. The spectroscopic factors obtained from these overlaps can be significantly different from the predictions of conventional shell models like that of Cohen and Kurath.

A recent test of these predictions is shown in Fig. V-6, where the ${}^6\text{He} + p|{}^7\text{Li}$ overlaps were used in a Coulomb distorted wave impulse approximation (CDWIA) analysis of previously unpublished

${}^7\text{Li}(e,e'p){}^6\text{He}$ experiments performed at NIKHEF. Lapikás and Wesseling obtained spectroscopic factors to the 0^+ ground state of ${}^6\text{He}$ of 0.42(4) and to the 2^+ first excited state of 0.16(2), in excellent agreement with our predictions of 0.41 and 0.18, respectively. A letter reporting these results was recently published¹.

In contrast to the proton knockout, we predict there should be significantly less quenching in the ${}^7\text{Li}(e,e'n){}^6\text{Li}$ reaction. We have provided our overlaps to an experimental group at MIT, and they are currently studying the feasibility of such an experiment with the new BLAST detector. We have also carried out initial calculations of overlaps in ${}^9\text{Be}$, which is the next stable target above ${}^7\text{Li}$, and we have predicted spectroscopic factors involving ${}^7\text{He}$, which is being developed as a radioactive beam at ATLAS.

*NIKHEF

¹L. Lapikás, J. Wesseling, and R. B. Wiringa, Phys. Rev. Lett. **82**, 4404 (1999).

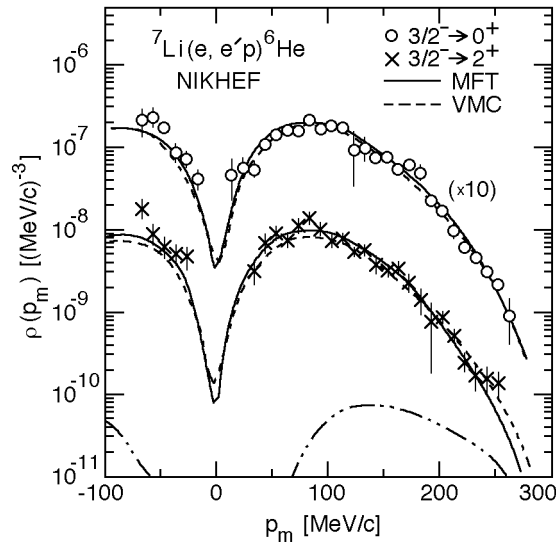


Fig. V-6. Experimental momentum distributions for the transitions to the ground state (circles) and first excited state (crosses) in the reaction ${}^7\text{Li}(e,e'p){}^6\text{He}$, compared to DCWIA calculations with meanfield (MFT) and variational (VMC) wave functions.

b.5. Radiative Capture Reactions for Astrophysical Applications (R. B. Wiringa and K. Nollett*)

Radiative capture reactions play a major role in many astrophysical processes, including primordial nucleosynthesis and stellar evolution. We are using the many-body quantum Monte Carlo wave functions discussed above to study radiative capture reactions involving light p-shell nuclei. Our first project is to obtain the low-energy cross section for ${}^4\text{He}(d, \gamma){}^6\text{Li}$. This reaction is the primary source of ${}^6\text{Li}$ in the big bang. The dominant nuclei synthesized in the big bang are ${}^2\text{H}$, ${}^3\text{He}$, ${}^4\text{He}$, and ${}^7\text{Li}$. Trace amounts of ${}^6\text{Li}$ should also have been made, although a primordial abundance has not yet been unambiguously identified in astronomical observations. The cross section at keV energies is sufficiently small that laboratory experiments have only established an upper bound, which could be orders of magnitude too high.

Our QMC wave functions are good for bound states, but are not as well developed for scattering states. Hence, we evaluate the appropriate electromagnetic matrix elements (primarily E2, E1, and M1) between a ${}^6\text{Li}$ ground state and a correlated n - d pair, which is then folded with a continuum n - d wave function obtained from a suitable optical potential. One of the interesting challenges has been to find ways of Monte

Carlo sampling in the tail of the ${}^6\text{Li}$ ground state where most of the capture reaction will take place. We have also developed an improved variational wave function for ${}^6\text{Li}$ that at long range has the form of n and d clusters with the empirical separation energy. At present, we are able to reproduce the observed E2 cross section from the 3^+ resonance at 0.7 MeV to beyond 3 MeV, but our E1 cross section in the same regime, which is an order of magnitude smaller, is two times too large compared to experiment, although the experimental data has sizeable error bars. At the capture energies of interest for primordial nucleosynthesis, the E1 and E2 contributions are about equal.

We also expect to study a number of other interesting radiative capture reactions such as ${}^4\text{He}({}^3\text{H}, \gamma){}^7\text{Li}$ and ${}^4\text{He}({}^3\text{He}, \gamma){}^7\text{Be}$, which also play an important role in primordial nucleosynthesis, and for which the experimental uncertainties are $\sim 30\%$. A good warm-up exercise for these calculations will be the thermal neutron capture reactions ${}^6\text{Li}(n, \gamma){}^7\text{Li}$ and ${}^7\text{Li}(n, \gamma){}^8\text{Li}$, which should provide a good test of our many-body wave functions, and for which good experimental data is available.

*University of Chicago

b.6. Microscopic Calculation of A = 6–8 Weak Decays (R. B. Wiringa and R. Schiavilla*)

Initial variational Monte Carlo calculations were made for the weak decays of ${}^6\text{He}$, ${}^7\text{Be}$, ${}^8\text{He}$, ${}^8\text{Li}$, and ${}^8\text{B}$. The variational wave functions were obtained for our standard Hamiltonian containing the Argonne v_{18} two-nucleon potential and the Urbana IX three-nucleon potential. Consistent two-body axial current operators tuned to reproduce ${}^3\text{H}$ β -decay are included in the evaluations.

Our calculated Gamov-Teller (GT) matrix element for ${}^6\text{He}(\beta^-){}^6\text{Li}$ is too large by 5%, while those for ${}^7\text{Be}(\beta^-){}^7\text{Li}$ and ${}^7\text{Be}(\beta^+){}^7\text{Li}^*$ are 5% too low, compared to experiment. The two-body axial current contributes only a 1% increase in $A=6$ and 3% in $A=7$. The branching ratio ${}^7\text{Li}^*/{}^7\text{Li}$ is 10.2% compared to the

experimental 10.5%. We are currently studying the sensitivity of these results to changes in the variational wave function, and plan to evaluate mixed estimates with the more precise GFMC wave functions in the near future. Nevertheless, the status of these *ab initio* calculations of $A=6-7$ weak decays looks quite satisfactory.

The situation for $A=8$ weak decays is much more difficult. While the $A=6-7$ decays are between states of predominantly the same spatial symmetry, the ${}^8\text{Li}$ and ${}^8\text{B}$ decays involve transitions from the $2^+[31]$ ground states to the $2^+[4]$ first excited state of ${}^8\text{Be}$, which is in fact a fairly broad resonance.

*TJNAF and Old Dominion University

The impulse approximation gives only 39% of the experimental GT matrix element; the two-body axial current is relatively more important here, but only boosts our result to 43%. The ${}^8\text{He}(\gamma){}^8\text{Li}$ decay proceeds from the $0^+[22]$ ground state to several $1^+[31]$ excited states. Again, we get less than 50% of the measured GT matrix element to the lowest ${}^8\text{Li}$ state;

however, in the ${}^8\text{He}$ decays, the experimental data is less complete. Again, we will be investigating alternate variational wave functions and computing GFMC mixed estimates in the near future. However, these suppressed $A=8$ decays will probably require additional physics input to reach a satisfactory state.

b.7. Single Particle Energies (A. R. Bodmer and Q. N. Usmani*)

After some revisions, this work was published with the above title.¹ We make microscopic calculations of the single particle energies B of hypernuclei (HN) in terms of N and NN potentials, which are phenomenological, but based on pion-exchange considerations. We also include a purely phenomenological space-exchange component in the N potential. Since the data for the HN range from C to ${}^{208}\text{Pb}$ realistic few-body calculations are not feasible. Our procedure is then based on a local density approach where the binding $D(\rho, k)$ of a hyperon of momentum k to nuclear matter of density ρ is calculated with the Fermi hypernetted chain (FHNC) method for densities $\rho \lesssim \rho_0$ where ρ_0 is the density of normal nuclear matter. From this we then obtain $D(\rho)$ the binding for $k = 0$, and $m^*(\rho)$ the effective mass. We also obtain corresponding effective N and NN potentials, which by suitable folding into the core-nucleus density distribution obtained from electron-scattering data, gives the ρ -core potential $U(\rho)$. This folding procedure is essential to obtain finite range effects due to the interactions, which play an important role especially for lighter and medium-heavy HN. The Schrodinger equation with $U(\rho)$ and $m^*(\rho)$ is then solved to obtain the B for the HN and angular momenta of interest. Another change compared to our earlier work is that we now use only a dispersive NN potential for which we can make reliable calculations, which so far has not been achieved for the two-pion exchange NN potential. However, we include a phenomenological dependence for the strength W of the dispersive NN potential, which allows for a two-pion-exchange contribution. This dependence is such that the effective strength becomes more repulsive at larger densities, and implies that this strength becomes more repulsive for large mass number A since lighter HN have relatively more surface. Our best fits in fact

require a large ρ dependence. This then translates into an A -dependent strength for W , nicely consistent with variational Monte Carlo calculations of ${}^5\text{He}$ which require $W = 0.01$ MeV, whereas normal nuclear matter requires $W = 0.02$ MeV. Thus without a density dependence, *i.e.* with a constant W , not only are the fits worse than with a density dependence but they also cannot be reconciled with ${}^5\text{He}$. The probable interpretation is in terms of a dispersive plus two-pion exchange NN potential since the latter is known to give an attractive contribution for lighter HN as a result of the associated correlations, but is conjectured to give a less attractive and possibly even a repulsive contribution for larger ρ , and hence for heavier HN. $D(\rho)$ has a saturation behavior, already previously known, with a maximum as a function of ρ , resulting from the interplay of the attractive contribution of the N forces, very approximately proportional to ρ , and the repulsive NN contribution very approximately proportional to ρ^2 . The effect of the density dependence of the effective strength W is to produce a sharper and larger maximum of $D(\rho)$ at a smaller $\rho = 0.125 \text{ fm}^{-3}$ than without the density dependence with the maximum at $\rho = 0.15 \text{ fm}^{-3}$. For the well depth we obtain $D(\rho_0) = 29 \pm 1$ MeV, well consistent with earlier values. The exchange fraction of the N potential corresponds to $m^*(\rho_0) = 0.75 m$ and to a ratio of p - to s -state N potential strengths of 0.45 , with considerably less uncertainty than the value obtained from p scattering. We have also included charge-symmetry breaking which leads to a difference between the ρ -proton and ρ -neutron interactions. An important new result is that charge-symmetry breaking becomes quite significant for heavy HN with a large neutron excess, and has a strength very well consistent with the value we obtained in earlier work from the $A = 4$ HN.

*Universiti Putra Malaysia, ¹Q. N. Usmani and A. R. Bodmer, Phys. Rev. C **60**, 055215 (1999)

b.8. Core-Nucleus Distortion in Hypernuclei (A. R. Bodmer and Q. N. Usmani*)

We are continuing our study of the effects of the spherical distortion of the core nucleus by the Λ in a hypernucleus. The response of the core is determined by an appropriately chosen energy-density functional which depends on the nuclear compressibility and which gives a very good description of the nuclear binding energies. The forcing action of the Λ is determined by the nuclear density dependence of the binding in nuclear matter which is obtained from our

work on the Λ -single energies. Because of the strongly repulsive NN forces, this Λ binding saturates at a density not very much less than the central density of nuclei, and results in a core-nucleus distortion which is much less than would be obtained with only N forces. The effects of core distortion turn out to be small even for light hypernuclei. Our results justify the usual assumption that spherical core distortion effects are small and can mostly be neglected.

*Universiti of Putra Malaysia

C. NUCLEAR STRUCTURE AND HEAVY-ION REACTIONS

This research focuses on nuclear structure in unusual regimes: nuclei far from stability, and superdeformed nuclei at high spin. We also study heavy-ion reactions near the Coulomb barrier. Much of this work is closely tied to experiments performed at ATLAS and at radioactive-beam facilities.

Our studies of drip-line nuclei focus on breakup reactions induced by the Coulomb and nuclear fields from a target nucleus. A critical issue is to develop a realistic description of breakup mechanisms as a necessary tool for extracting or testing the nuclear structure properties of drip-line nuclei. An example of particular interest to solar neutrino physics is the low-lying $E1$ strength of ${}^8\text{B}$ which determines the radiative proton capture on ${}^7\text{Be}$ in the sun. We have developed a single-particle model which reproduces the low-lying dipole strength of ${}^8\text{B}$, extracted in recent Coulomb dissociation experiments. We have tested the model against other observables that are sensitive to the size of the valence proton state. Thus we find that the model is consistent with the measured cross sections of the predominantly nuclear-induced breakup on a carbon target.

We have extended our studies of drip-line nuclei to include the structure and decay of deformed proton emitters. This is described in a coupled-channels treatment of the particle-rotor model, supplemented with a Green's function technique. The calculation of decay rates is commonly performed by using complex energies. This is a difficult task because the decay widths of interest are extremely small. However, by employing the Green's function method it is sufficient to solve the coupled equations with an energy that is real. The results we obtain for the decay of low-spin states are quite encouraging in comparison to measurements. The decay from high-spin states, on the other hand, is much more difficult to predict. It is influenced by the Coriolis force, which is too strong without the effect of pairing.

Our studies of superdeformed nuclei, at both low and high spins, address the issues of possible new regions of superdeformation and hyperdeformation. Special emphasis is being put on the study of fission barriers at high spin, and the relation between fission barriers and the possibility of producing very extended nuclear shapes. Other areas of interest are the structure of heavy elements and superheavy elements, density dependence of two-body interactions, and the phenomenon of proton radioactivity. The techniques we use to study these problems are a deformed central potential approach for surveying nuclear structure over a large region, self-consistent mean-field calculations for more detailed studies of particular nuclides, and many-body wave functions when residual interaction effects are small and a mean-field approach is inadequate.

Much of our work is computer intensive and we are adapting our codes to exploit the massively parallel IBM SP supercomputer system at Argonne. The use of the SP system allows us to calculate energy surfaces as a function of angular momentum, using the Strutinsky method with cranking, in a four-dimensional deformation space consisting of quadrupole, octupole, hexadecapole, and necking degrees of freedom. We carried out studies of nuclear energy surfaces in nuclei with masses ranging from $A \sim 80$ to $A \sim 200$. We are analyzing these calculations to look for nuclei that are good candidates for experimental investigation of superdeformation. Our recent analysis of energy surfaces near $A=100$ suggests that very extended minima in several nuclides near ^{108}Cd are experimentally accessible. Experimental studies motivated by these calculations have led to the observation of a superdeformed band in ^{108}Cd . We have adapted our many-body code for parallel computer systems and have modified it so as to allow the use of general two-body matrix elements. We are using this code to study the nuclear structure of nuclides near the proton dripline. A complementary effort, in conjunction with J. L. Egido and L. M. Robledo, is also focused in this area. In the latter studies, we are using a Gogny interaction in the HFB approximation. We have completed an analysis of excited states in ^{256}Fm ; the heaviest nuclide for which there is extensive spectroscopic information on non-intrinsic excited states. The pairing force strength obtained from this analysis will improve the reliability of future theoretical studies of superheavy elements.

c.1. Systematic Study of ^8B Breakup Cross Sections (H. Esbensen and K. Hencken*)

The low-lying E1 response of ^8B has recently been extracted from measurements of the $^8\text{B} \rightarrow ^7\text{Be} + p$ breakup on a Pb target, namely, from longitudinal momentum distributions of ^7Be fragments¹, and from the decay energy spectrum². Since the strength of the low-lying E1 response is closely related to the mean-square-radius of the valence proton in ^8B , it is useful to investigate whether it is consistent with other observables that are sensitive to the size of the valence proton density. In this work we have focussed on the one-proton removal cross section.

We describe the valence structure of ^8B in a two-body model, with an inert ^7Be core and a weakly bound proton. The nuclear induced breakup of ^8B is calculated in the eikonal approximation, whereas Coulomb dissociation is calculated to first order. We assume that the core of ^8B is identical to a free ^7Be nucleus and calibrate the core-target interaction so that the measured ^7Be interaction cross sections are reproduced.

The calculated one-proton removal cross sections are shown in Fig. V-7 for different targets as functions of

the beam energy. The solid curves are the results we obtain when we adjust the structure model to reproduce the recently extracted E1 strength. The uncertainty in the extracted E1 strength and also in our calibration of the core-target interaction results in a total uncertainty of about 10% in the predicted cross sections. Thus we conclude that the predictions are consistent with measurements on a C target (except the one at 40 MeV/u, which falls outside the systematics). This is a nice result because the ^8B breakup on C is mainly induced by nuclear interactions. The dashed curves are based on a model that gives a 20% smaller E1 strength; the predictions of this model are clearly inconsistent with the C data.

The predicted cross sections on high-Z targets are larger than the data. This is ascribed to approximations we have made. Thus we treat the Coulomb and nuclear induced breakup as independent processes. Moreover, the radial dependence of the Coulomb form factors that we have used assumes that the target nucleus does not penetrate the valence proton density. A way to improve our description for high-Z targets is discussed below. This work has been submitted for publication.

*University of Basel, Switzerland

¹B. Davids *et al.*, Phys. Rev. Lett. **81**, 2209 (1998)

²N. Iwasa *et al.*, Phys. Rev. Lett. **83**, 2910 (1999)

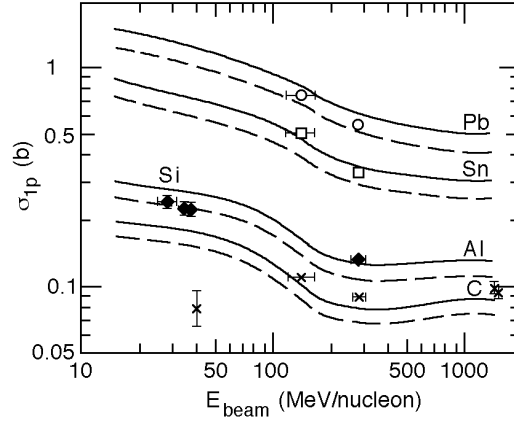


Fig. V-7. Calculated and measured one-proton removal cross sections for ${}^8\text{B}$ on C, Al, Si, Sn, and Pb targets, as functions of the ${}^8\text{B}$ beam energy. The solid curves are based on a model that reproduces the E1 strength extracted from recent experiments^{1,2}. The dashed curves are based on a model that produces a 20% smaller E1 strength.

c.2. Coulomb-nuclear Interference in Breakup Reactions of ${}^8\text{B}$ (H. Esbensen)

The analyses of measured decay-energy spectra of ${}^8\text{B}$ have all lead to the conclusion that the E2 strength is strongly quenched¹. The origin of the quenching has not yet been fully explained. Higher-order processes play a role at low beam energies² but they should be much less important at high energies. It was therefore surprising that the analysis of a measurement at 254 MeV/u also required a strong quenching of the E2 strength¹. In this work I try to explain why a quenching is necessary even at high energy.

A general description of first-order Coulomb dissociation can be made in the distorted wave Born approximation. At high energies, it is sufficient to use a semiclassical description of the relative motion of projectile and target. The distorted waves, which are generated by nuclear interactions with the target, can be estimated in the eikonal approximation, whereas Coulomb excitation is treated to first-order. From these approximations one can derive the following expression for the decay energy spectrum:

$$\frac{d}{dE} = \frac{\mu}{\hbar^2 k} 2 \text{ bdb} \left| \left\langle \begin{matrix} k l j m \\ l j m \end{matrix} \left| \left(e^{i N} - 1 \right) + e^{i N} C \right| \begin{matrix} g s \\ g s \end{matrix} \right\rangle \right|^2.$$

Here N is the nuclear eikonal phase, which depends on the impact parameter and the position of the valence proton with respect to the ${}^7\text{Be}$ core. The first term, *i.e.* the matrix element of $(e^{i N} - 1)$ between the ground state of ${}^8\text{B}$ and continuum states, is responsible for nuclear diffraction dissociation. The second term

contains the operator C , which is responsible for the first-order Coulomb dissociation. It is multiplied by the eikonal factor $e^{i N}$, which suppresses the Coulomb dissociation operator when the valence proton penetrates the target nucleus and gets absorbed. The combined expression includes the interference between the Coulomb and nuclear induced breakup.

¹N. Iwasa et al., Phys. Rev. Lett. **83**, 2910 (1999)

²H. Esbensen and G. F. Bertsch, Nucl. Phys. **A600**, 37 (1996)

The numerical calculation of the above expression is much more complicated and time-consuming than the 'conventional' calculation of Coulomb dissociation in which one ignores the influence of nuclear processes; they enter only via a cutoff in the integration over impact parameters. The conventional analyses also employ a multipole expansion of the Coulomb field from the target, which assumes that the target nucleus

does not penetrate the density of the valence proton. This assumption is reasonable for tightly bound nuclei but it is questionable for a loosely bound nucleus like ^8B . By using the correct multipole expansion of the Coulomb field, and including the influence of the nuclear field as described above, one may be able to explain the empirical quenching of the Coulomb dissociation. This work is in progress.

c.3. Calculations of Proton Decay Rates of Spherical and Deformed Nuclei

(C. N. Davids and H. Esbensen)

We have used a Green's function technique, based on the Gell-Mann-Goldberger transformation, to show that the "distorted wave" decay rates calculated by Aberg¹ and the "exact" decay rates calculated by Maglione² for spherical proton emitters are mathematically equivalent^{3,4}. Numerically the two methods give half-

lives agreeing to within 0.005%. We have also extended the Green's function technique to cover the case of deformed proton emitters^{3,4}, and shown that the decay rates calculated by Maglione *et al.*² and Kadmensky and Bugrov⁵ are equivalent.

¹S. Aberg, P. B. Semmes, and W. Nazarewicz, Phys. Rev. C **56**, 1762 (1997); Phys. Rev. C **58**, 3011 (1998)

²E. Maglione et al., Phys. Rev. Lett. **81**, 538 (1998); Phys. Rev. C **59**, R589 (1999)

³C. N. Davids and H. Esbensen, Proceedings of the International Symposium on Proton-Emitting Nuclei, 6-9 October 1999, Oak Ridge, TN, AIP Conference Proceedings, in press (2000)

⁴C. N. Davids and H. Esbensen, Physical Review C in press (2000)

⁵V. P. Bugrov and S. G. Kadmensky, Sov. J. Nucl. Phys. **49**, 967 (1989), S. G. Kadmensky and V. P. Bugrov, Phys. of Atomic Nuclei **59**, 424 (1996)

c.4. Coupled-channels Treatment of Proton Emission (H. Esbensen and C. N. Davids)

Measurements of the proton decay of deformed nuclei beyond the proton drip line have previously been analyzed in a particle-rotor model, making use of several approximations. Thus the wave functions of the decaying states have been calculated by diagonalizing a deformed Hamiltonian in a spherical, single-particle basis. Moreover, this was done in the adiabatic limit, where the excitation energies of the core are set to zero. Since the decay rate is extremely sensitive to the energy of the emitted protons, we decided to improve the description by adopting the coupled channels approach, which allows us to include non-zero core excitation energies. Moreover, the radial wave functions are automatically generated by solving a set of coupled radial equations.

The decay rate of a resonance is determined by the amplitudes of the asymptotic radial wave functions at large distances. It is, however, very difficult to calculate the radial wave functions of a resonance accurately out to large distances, where the long-range Coulomb quadrupole coupling can safely be ignored. It requires that the resonance energy has been determined with extremely high precision, much better than 1 eV. A simple way to overcome this problem is to solve the coupled equation out to 10 to 20 fm. One can then use the Green's function method (GFM)¹ to extrapolate the wave function out into the asymptotic region and include the effect of the long-range Coulomb coupling to first order.

An example is illustrated in Table IV-3. for the decay from the $3/2^+$ ground state of ^{131}Eu to the 0^+ ground state and to the excited 2^+ and 4^+ states of the ^{130}Sm daughter nucleus. The first line gives the measured decay widths². The second line gives the results of the coupled channels approach, which are in fair agreement

with the measurement. The third line gives the results we obtain in the adiabatic limit. It is seen that the decay widths to the 2^+ and 4^+ states are grossly overestimated compared to the coupled-channels results.

Table V-3. Decay widths (in units of 10^{-20} MeV) for the $3/2^+$ ground state of ^{131}Eu to the 0^+ ground state and the 2^+ and 4^+ excited states of ^{130}Sm .

	0+	2+	4+
Experiment [2]	1.71	0.54	-
Coupled-channels method	1.83	0.99	3.16×10^{-8}
Adiabatic limit	2.05	83.9	13.7
Adiabatic limit + GFM	2.05	1.01	2.83×10^{-8}

The Green's function method can also be used to improve the results obtained in the adiabatic limit because it allows us to implement the correct energy of the emitted proton, when the daughter nucleus ends up in an excited state. The results we obtain are given in the fourth line. The decay widths to the 2^+ and 4^+

states are now strongly reduced but they are close to the values obtained in the coupled-channels calculation. The methods we have developed will be used to extract information about the structure of proton-rich nuclei from measurements of the decay rates and energies of the emitted protons.

¹C. N. Davids and H. Esbensen, Phys. Rev. C in press (2000)

²A. A. Sonzogni et al., Phys. Rev. Lett. **83**, 1116 (1999)

c.5. Many-body Wave Functions (R. R. Chasman)

We are continuing the development of many-body variational wave functions that put pairing and particle-hole two-body interactions on an equal footing. The variational parameters are calculated with an iteration procedure. The complexity of the wave functions depends only on the number of levels included in the valence space, but does not depend on the number of nucleons in the system. In these wave functions, we conserve particle number and parity strictly by projecting states of good particle number and parity before carrying out the variational calculations. We have added a cranking term to the many-body Hamiltonian and modified the projection procedure to get states of good signature before variation. This

allows us to study pairing collapse as a function of angular momentum. We have also extended the program to calculate spectroscopic factors involved in proton decay. This is useful for studies of nuclides near the proton drip line.

By using residual interaction strengths (*e.g.* the quadrupole interaction strength or pairing interaction strength) as generator coordinates, one gets many different wave functions; each having a different expectation value for the relevant interaction mode. Such wave functions are particularly useful when one is dealing with a situation in which a configuration interaction treatment is needed. This is particularly true

for an adequate treatment of pairing at high spin as well as for instances in which the single-particle level density is low. Because the same basis states are used in the construction of all of the many-body wave functions, it is possible to calculate overlaps and interaction matrix elements for the many-body wave functions obtained from different values of the generator coordinates (which are not in general orthogonal) easily. The valence space can contain a very large number of single-particle basis states, when there are constants of motion that can be used to break the levels up into groups.

Wave functions of this sort become more realistic as the size of each of the groups is increased. To increase this size, we have parallelized our code to run on the SP computer system. We have also modified our codes to handle arbitrary two-body matrix elements. This latter feature allows us to include Coulomb matrix elements easily. Together with J.L. Egido and L.M. Robledo, we have developed subroutines for calculating Gogny interaction matrix elements and Coulomb matrix elements for this many-body code.

As is the case with most non-linear problems, the results are sensitive to the choice of starting values for the variational parameters. We have been examining choices of starting points and other strategies for dealing with this problem. We have introduced a pseudo-annealing procedure, by adding a one-body off-

diagonal matrix element to the interaction and then let the system cool slowly. This is of limited value. We have also constructed a starting wave function by maximizing its overlap with a configuration-interaction solution and then using this wave function as a new starting point for our minimization procedure. This has been moderately successful.

We have been more successful in improving our minimization procedure with some other strategies. First of all, we have found that making the changes in the variational amplitudes for proton and neutron amplitudes inversely proportional to the magnitude of the respective pairing correlations is very useful, when going from one iteration to the next. This helps the proton and neutron amplitudes converge at the same rate and we get improvements in the energy. We have found that our many-body wave functions are relatively resistant to large-scale structural changes so long as the relative phases of the variational amplitudes are not changed. We have been able to utilize this feature to get improvements in many-body wave functions by taking the results of a minimization and then restarting the iterative procedure with a wave function in which all positive amplitudes are replaced by +1 and all negative amplitudes are replaced by -1. This approach is particularly valuable for improving the energies of wave functions in metastable minima, because the new trial functions do not fall into the absolute minimum.

c.6. Very Extended Shapes in Nuclei (R. R. Chasman)

In the past few years, large computer resources have become available on the massively parallel processor IBM SP system at Argonne, in addition to the resources provided by NERSC. We have parallelized the code used to calculate single-particle spectra to exploit the SP system and have devoted a large part of our efforts to calculating energy surfaces in a four-dimensional shape space that includes reflection asymmetric shapes. We study the nuclear energy surfaces as a function of mass, charge, shape and angular momentum, using the Strutinsky method. In this approach, one makes quantum corrections to a smooth liquid drop behavior using the calculated single-particle energy levels. In earlier studies, we found that it is often not sufficient to

use only quadrupole and hexadecapole deformations to describe very extended reflection-symmetric nuclear shapes. When we added a necking degree of freedom, we found previously unknown minima. These minima are characterized by very extended capsule shaped nuclei with axis ratios of 2.2:1 in the A=180 mass region. We have now added octupole deformation to this shape space. The inclusion of these two degrees of freedom in our shape space substantially increases our ability to describe nuclear shapes compared to a typical shape space consisting only of quadrupole and hexadecapole deformations. As parity is no longer a good quantum number when octupole deformation is included, the size of the matrices that we diagonalize

¹R.R. Chasman, Workshop on the Science for an Advanced ISOL Facility, (1997) p. 69

²R.R. Chasman, PHY-9018-TH-98

³R.R. Chasman, Phys. Rev. Lett. **80**, 4610 (1998)

⁴R.R. Chasman Phys. Lett. **B219**, 227 (1989)

is doubled. In a typical calculation, we diagonalize matrices that are 600×600 . Several thousand such diagonalizations are needed to determine energy surfaces.

There remains a need to test calculated fission barriers and to generally understand nuclear properties at the highest spins. Using the four-dimensional deformation space described above, we have analyzed the high-spin energy surfaces of the $N=86$ isotones going from Sn ($Z=50$) to Dy ($Z=66$). There is a high spin superdeformed minimum in all of these nuclides ($\sim 1.85:1$ axis ratio) that becomes yrast at high spin. These shapes are well known experimentally in the Dy region.

We find that as the proton number decreases from $Z=66$ to $Z=50$, the fission barrier increases by roughly 10 MeV at a given angular momentum. The superdeformed minimum associated with $N=86$ is present for both Sn and Dy. This result suggests that we can extend the study of nuclear properties at extreme deformations to a new regime of angular momenta, with the availability of radioactive nuclear beam facilities. A preliminary version of this work has been published.¹

c.7. Single-Particle States in the Heaviest Elements (R. R. Chasman and I. Ahmad)

The search for superheavy elements has been a major theme of nuclear structure research for the past twenty years. Theoretical predictions of the stability of superheavy elements depend crucially on the single-particle energy level spacings in the vicinity of 114 protons and 184 neutrons. Our approach is to learn as much as possible about these levels from spectroscopic studies of nuclides in the $A=250$ region. This is possible because there are members of the relevant spherical multiplets that drop rapidly in energy with increasing deformation, and are fairly close to the ground state in the strongly deformed nuclides near $A=250$. The orbitals that are important for fixing the shell corrections near $N=184$ are the $h_{11/2}$, $j_{13/2}$ and $k_{17/2}$ spherical states. For each of these spherical orbitals, there is a corresponding deformed orbital whose energy in the $A=250$ region is quite sensitive to one of these spherical states, *e.g.* the $1/2-[761]$ orbital

We have extended our high spin Strutinsky calculations² to nuclei in the $A=100$ mass region. Many of the very extended minima that we find will be accessible with projectiles produced at an exotic beam facility. However, our calculations show very extended minima in nuclides in the vicinity of ^{108}Cd that are accessible using existing facilities. Recent experiments, inspired by these calculations, show a superdeformed rotational band in ^{108}Cd .

Several odd-parity excited states have been found in the superdeformed minima of the Hg region. Because of their low excitation energies, it had been thought that these states are very collective. Making use of a particle number conserving treatment of pairing, we found³ that one can calculate the excitation energies of these states quite well as simple broken pair excitations; using conventional pairing force strengths and the single-particle levels that were obtained when superdeformation in this mass region was first⁴ predicted. The transition matrix elements connecting these excited states to the superdeformed yrast band remain to be explained.

We are analyzing nuclides in the region $70 < A < 100$, searching for very extended minima.

that has already been identified in ^{251}Cf is quite sensitive to the energy of the spherical $j_{13/2}$ orbital. The position of the $1/2+[880]$ deformed orbital is very sensitive to the single particle energy of the $k_{17/2}$ spherical state. We have calculated signatures for the low-lying states in ^{251}Cf and the calculated energies and signatures are in good agreement with the experimentally observed (d,p) spectrum. We expect to see the high-J states in an (α , ^3He) transfer reaction. As a ^{250}Cf target is not available, we have studied the high-J states in ^{249}Cm , which is an isotone of ^{251}Cf . The (α , ^3He) experiment has been carried out and two high-J peaks have been observed at ~ 1.6 and 1.9 MeV. These peaks are candidates for the $1/2+ [880]$ band. Additional coincidence studies will be needed to make a definitive assignment. This study¹ has been published.

¹I. Ahmad *et al.*, Nucl. Phys. **646**, 175 (1999)

²R. R. Chasman and I. Ahmad, Phys. Lett. **B392**, 255 (1997)

³I. Ahmad, R.R. Chasman and P. R. Fields, Phys. Rev. C (accepted for publication)

Using the Strutinsky method, we found² that we could get very good agreement with the known low-lying levels in ²⁵¹Cf using a Woods-Saxon potential. We have used the potential parameters generated from this fit to study the stability of superheavy elements. To determine potential parameters for protons in the heavy elements, we utilized data from our spectroscopic studies of ²⁵⁵Md. These studies show the 1/2-[521] orbital to lie above the 7/2-[514] orbital, but the magnitude of the energy difference is not known. Determining the potential in this way, we extrapolate directly to the superheavy element region. As the usual zero-point correction to mass estimates is questionable in that it treats only the quadrupole deformation mode, we replaced this correction in our mass estimates by a term that depends quadratically on the sum of the proton and neutron shell corrections. This correction is easy to evaluate and gives quite reasonable corrections where masses are known. Using the potential parameters derived from the heaviest elements for which there is detailed spectroscopic information, we find that our calculated lifetimes are sufficiently long so as to be able to observe elements at least through Z=120.

In our analysis, we have assumed that the 1/2-[521] orbital lies just above the 7/2-[514] orbital in ²⁵⁵Md. In fact, this level spacing is not yet known. Our estimates of superheavy element stability will be affected by the experimental value of this level spacing. We hope to determine this spacing through experimental studies,

c.8. Studies of Nuclear Energy Surfaces (R. R. Chasman, J. L. Egido,* and L. M. Robledo*)

This collaborative research program is focused on the study of nuclear energy surfaces, with an emphasis on very deformed shapes using two complementary methods: 1) the Strutinsky method for making surveys of mass regions and; 2) Hartree-Fock calculations using a Gogny interaction to study specific nuclei that appear to be particularly interesting from the Strutinsky method calculations. The great advantage of the Strutinsky method is that one can study the energy surfaces of many nuclides (~300) with a single set of

and thereby refine our estimates of superheavy element lifetimes. Another important feature in determining the binding energy of superheavy elements is the magnitude of the pairing interaction strength.

We have recently completed a study³ of excited states in ²⁵⁶Fm, which is the heaviest nucleus in which excited non-rotational states have been observed. We have used the I=7 negative parity state at 1426 keV in this nuclide to adjust the proton pairing interaction strength. Our calculated spectrum for other proton broken pair states is in good agreement with those that have been observed, and we predict many other such states between 1 and 2 MeV. Pinning down the proton pairing strength, in the heaviest nuclide where there is sufficient data to do so, improves the reliability of predictions of the stability and structure of yet heavier elements.

Additionally, we have studied³ the decay of ²⁵⁵Md to determine low-lying single-particle state assignments in ²⁵⁵Fm and ²⁵¹Es. Through studies such as these, we hope to get an accurate picture of nuclear structure on both sides of the deformed neutron single particle gap at N=152 and the deformed proton gap at Z=100.

At present, we are analyzing excited states in ²⁵¹Cf populated in the alpha decay of ²⁵⁵Fm. This will give further insight into nuclear structure beyond the N=162 deformed gap.

calculations. Although, the Hartree-Fock calculations are quite time consuming relative to the Strutinsky calculations, they determine the shape at a minimum without being limited to a few deformation modes. We have completed a study of ¹⁸²Os using both approaches. In our cranked Strutinsky calculations, that incorporate a necking mode deformation in addition to quadrupole and hexadecapole deformations, we found three well separated, deep, strongly-deformed minima. The first is

*Universidad Autonoma de Madrid

¹R. R. Chasman and L.M. Robledo, Phys. Lett. **B351**,18 (1995)

²J. L. Egido, L.M. Robledo and R.R. Chasman, Phys. Lett. **B393**, 13 (1997)

³L. M. Robledo, J.L. Egido, and R.R. Chasman, Proceedings of the Conference on Nuclear Structure at the Limits, Argonne National Laboratory, Argonne, IL, July 22-26 (1996) p. 124

⁴C. N. Davids *et al.*, Phys. Rev. Lett. **76**,592 (1996)

characterized by nuclear shapes with axis ratios of 1.5:1; the second by axis ratios of 2.2:1 and the third by axis ratios of 2.9:1. We also studied this nuclide with the density-dependent Gogny interaction at $I=60$ using the Hartree-Fock method and found minima characterized by shapes with axis ratios of 1.5:1 and 2.2:1. A comparison of the shapes at these minima, generated in the two calculations, shows that the necking mode of deformation is extremely useful for generating nuclear shapes at large deformation that minimize the energy. The Hartree-Fock calculations are being extended to larger deformations in order to further explore the energy surface in the region of the 2.9:1 minimum.

With the recent availability of large computer resources on the SP system at Argonne, together with the continued availability of computing resources at NERSC, it is feasible to carry out Strutinsky calculations on a large four-dimensional grid in a deformation space that includes octupole deformation in addition to quadrupole, hexadecapole and necking deformations. We are carrying out this study of the $A\sim 180$ region concentrating on the questions: 1) how do the inclusion of necking and reflection-asymmetric degrees of freedom modify nuclear energy surfaces and; 2) how soft are the many, known, very-deformed nuclear shapes in this region to octupole deformation?

We have completed¹ the first phase of these studies, using the Strutinsky method to calculate nuclear energy surfaces in the four-dimensional space discussed above. Comparing the results obtained with and without octupole deformation, we found major modifications of the energy surface in many nuclei in the region around ^{176}W . These effects are strong at all values of the angular momentum. There are reductions of the total energy of ~ 7 MeV for the necked-in shapes at the largest deformations. This feature can be understood in terms of incipient fission fragments. The reflection-asymmetric shape is necked-in in such a way as to exploit the large shell corrections associated with a strongly deformed fragment in the vicinity of ^{100}Zr and a spherical fragment in the vicinity of ^{80}Zr . The symmetric necked-in shape at these large deformations corresponds to two strongly-deformed incipient fission fragments near $A=90$ and is not favored. The effects are huge here, compared to typical octupole deformation energy gains of less than 1 MeV.

As in the case for Strutinsky method calculations, the introduction of reflection asymmetry doubles the basis space that must be used in Hartree-Fock calculations.

We have extended the Hartree-Fock codes to allow us to calculate the properties of very-deformed reflection asymmetric shapes, using a one-center basis. We have finished a calculation² of the energy surface of ^{176}W at $I=0$, using the Gogny interaction. In these calculations, we also found a substantial lowering of the fission barrier when reflection asymmetric shapes are allowed. At $I=0$, where the Hartree-Fock calculations were carried out, the fission barrier is lowered by 4.5 MeV when reflection asymmetric shapes are included. At $I=0$, the reduction is 6.2 MeV in the Strutinsky calculations. The agreement between these two very different methods is impressive. In the Hartree-Fock calculations, the asymmetric division is into fission fragments of ^{66}Ni and ^{110}Pd .

We have recently broadened the area of our comparative studies to include low-spin studies in the neutron-deficient Pb region. In addition to HFB and Strutinsky calculations, we are applying the many-body wave functions discussed above, which go beyond mean-field approximations.

The neutron-deficient nuclides ($N < 110$) in the Pb region have states that are characterized by three distinct shapes; spherical, prolate and oblate. In the oblate and prolate states, there are low-lying single-particle states derived from spherical states on both sides of the $Z=82$ single-particle gap. Although this gap is roughly 4 MeV, there are states within a few hundred keV of ground in the neutron-deficient $\text{Tl}(Z=81)$ and $\text{Bi}(Z=83)$ isotopes that would be at ~ 4 MeV excitation, in the simplest single-particle picture. In addition, proton emission has been observed in the nuclide ^{185}Bi . We are making calculations of the properties of nuclides in this region using our many-body wave functions. In addition, we are also studying many of these same nuclides using the Gogny interaction in the HFB approximation.

Proton emission has been observed⁴ in the light Pb nuclei. It seems that one might hope to use this phenomenon to extract some interesting spectroscopic data on nuclear shapes and orbitals in much the same way that one gets spectroscopic information through single-nucleon transfer reactions such as (d,p) and (d,t) reactions. In order to explore this possibility, we have developed a treatment of proton-emission spectroscopic factors using many-body wave functions. In the case that we have studied (^{185}Bi ^{184}Pb), the energetics of the reaction are such that only the ground state is populated. We calculate a very small spectroscopic factor for the proton decay to the ground state. The small spectroscopic factor is largely due to the shape

difference between the deformed decaying state in ^{185}Bi and the ground state of ^{184}Pb , which is spherical. To understand this spectroscopic factor, it is necessary

to have good wave functions for the initial and final states. Our systematic study of this region should provide us with improved wave functions.

D. ATOMIC THEORY AND FUNDAMENTAL QUANTUM MECHANICS

d.1. Interactions of High-Energy Photons with Matter (M. Inokuti)

In support of experimental work in atomic physics with the use of synchrotron radiation, theoretical studies are being conducted on the physics of Compton scattering by bound electrons, focusing on topics selected in view of basic importance, timeliness, and potential in applications.

When the photon energy greatly exceeds the binding energy of an electron, the effect of electron binding to an atom is largely understood in the framework of an impulse approximation, which accounts for the momentum of an electron at the instant of the Compton scattering. However, the physics remains to be explored for a more general case, where full details of atomic structure, described for instance in terms of the

Green's function, need to be considered.¹ For a hydrogen-like atom, or within a simple-electron approximation, full analysis of the binding effect is theoretically feasible. Efforts are being made to elucidate basic points of the physics involved and to suggest items for experimental exploration.

Work on the Compton scattering by liquid water has been completed. Results of recent measurements by a group at Sendai were compared closely with an earlier semi-empirical determination of the Bethe surface (the strength of the Compton scattering plotted as a function of both energy transfer and momentum transfer), within the impulse approximation and a reasonably good agreement was found¹.

¹M. Dingfelder and M. Inokuti, *Radiat. Environ. Biophys.* **38**, 93 (1999)

d.2. Interactions of Fast Charged Particles with Matter (M. Inokuti)

Stopping power, the total yield of ionization, its fluctuation, ionization cross sections, and other quantities related to the energy loss of fast charged particles penetrating through matter are important in many applications such as the detection of particles and the analysis of their charges and kinetic energies. A review of the current understanding of "W, F, and I: Three quantities basic to radiation physics" was published¹.

A monograph² on "Fundamentals of Plasma Chemistry" was edited. It contains nine articles reviewing fundamental aspects of the processing of

material surfaces by use of low-temperature chemically active plasmas, including electron interactions with various atoms, molecules, and solid surfaces.

Another review on "Electron collision cross sections of atoms" has been produced for inclusion in a forthcoming volume on "Atomic Collisions" in the Landolt-Börnstein Numerical Data and Functional Relationships in Science and Technology, Springer-Verlag. This article reports on various cross sections for electron collisions with free atoms, and presents values recommended as best in the light of current knowledge.

¹M. Inokuti, in the proceedings of the International Symposium in Commemoration of Professor Doko's Seventieth Birthday, eds. S. Kubota and J. Kikuchi (Waseda University Press, Tokyo 1999) p. 1.

²M. Inokuti and K. H. Becker (eds), *Advances in Atomic, Molecular, and Optical Physics*, Vol. 43, Fundamentals of Plasma Chemistry, (Academic Press, San Diego 1999) 166 pages.

d.3. Stochastic Variational Approach to Quantum Mechanical Few-body Problems (Kálmán Varga)

The quantum mechanical few-body problem is of fundamental importance for all branches of microphysics and it has substantially broadened with the advent of modern computers. This book gives a simple, unified recipe to obtain precise solutions to virtually any few-body bound state problem and presents its application to various problems in atomic,

molecular, nuclear and solid state physics. The main ingredients of the methodology are wave function expansion in terms of Correlated Gaussians and optimization of the variational trial function by stochastic sampling. The book is written for physicists and, especially, for graduate students interested in quantum few-body physics¹.

¹Y. Suzuki and K. Varga, "Stochastic Variational Approach to Quantum Mechanical Few-body Problems", Springer-Verlag (Berlin Heidelberg, 1998).

d.4. Multipositronic Systems (Kálmán Varga)

Recent calculations have given the very surprising result that a positron can cling to a neutral atom. The simplest such positronic atom is the $\text{Li}e^+$. We have explored the possibility of the formation of stable atoms/ions containing two or more positrons. It is shown that the H^- and the Li^- ions can bind not only one but two positrons. The binding energies of these

double positronic atoms $E(\text{H}^-, e^+, e^+) = 0.57\text{eV}$ and $E(\text{Li}^-, e^+, e^+) = 0.15\text{eV}$ are somewhat smaller than those of their single positronic counterparts ($E(\text{HPs}) = 1.06\text{eV}$ and $E(\text{LiPs}) = 0.32\text{eV}$). We have also found that a proton and two Ps^- positronium ions where $\text{Ps}^- = (e^+, e^-, e^-)$, can form a bound system.¹

¹K. Varga, Phys. Rev. Lett. **83**, 5471 (1999)

d.5. Force-Free Interactions and Nondispersive Phase Shifts in Interferometry (M. Peshkin)

In earlier work, I sharpened an observation of Zeilinger to prove that force-free interactions in a Mach-Zehnder interferometer lead to nondispersive, *i.e.*, energy-independent, phase shifts. That result can be useful in interpreting the results of certain types of interferometry experiments. Recently, a photon-interferometry experiment and a proposed neutron-

interferometry experiment have been misinterpreted by their authors, who did not consider the nondispersivity test, as demonstrating a new kind of geometrical effect. I have corrected that interpretation and the ensuing discussion has led to a new proposed experiment. A Comment presenting this work has been accepted for publication by Foundations of Physics Letters.

d.6. A No-go Theorem for Matter-wave Interferometry with Application to Neutron Electric-Dipole Moment Experiments (M. Peshkin)

Work on this project has been completed. The no-go theorem addresses a recent proposal to measure the neutron electric-dipole moment (EDM) by novel interferometry techniques. Ultra-cold neutrons in a state described by some initial wave packet and polarized in the $+z$ (vertical) direction are to be exposed to a strong external electric field gradient in the x direction. The resulting force F_x on the EDM will cause the initial wave packet to evolve into the coherent sum of two spatially different partial wave packets, one with $x = +1$ and one with $x = -1$. The two partial wave packets will differ little, their centroids being separated in x by an amount proportional to the EDM and equal to some femtometers if the EDM equals 10^{-25} e-cm. The spatial separation is then to be changed to a separation in horizontal momentum by letting the neutrons fall under the influence of gravity and reflecting them from a mirror set at 45 degrees to the vertical, after which the neutrons are to bounce along a long horizontal beam tube extending in the x direction. As the neutrons proceed along the beam tube, the relative phase of the two partial wave packets is expected to grow because of their different central momenta. That relative phase growth, which is

proportional to the EDM and to the length of the beam tube, results in a rotation of the neutrons' polarization, to be measured at the end of the beam tube.

I have shown that if one measures the polarization in the most direct way, by catching the neutrons in a box and measuring the polarization at an instant, that will not work. The unitarity of the time evolution guarantees that the so-measured polarization will not change as the neutrons progress down the beam tube, contrary to semi-classical expectations. If, alternatively, one measures the polarization as the neutrons pass a place in the beam tube, then the rotation of the polarization, now time dependent, does grow proportionally to the length of the beam tube, but the expected rotation is too small to be measured in practice. In principle, separating the two wave packets by magnetic reflectors that act on the neutron's magnetic-dipole moment may enable an interferometric measurement of the EDM, but the practicalities of that scheme have not been investigated. A paper reporting this work has been accepted for publication in *Nuclear Instruments and Methods in Physics Research, Section A*.

d.7. Quantum Robots (P. Benioff)

Work on quantum robots was continued in 1999. A quantum robot is a mobile system with an on-board quantum computer and ancillary memory, output, and control systems. The quantum robot interacts with other quantum systems in its environment. The dynamics of the interaction is described by tasks that are alternating sequences of computation and action phases. Which type of phase is active depends on the state of the control system. Each computation phase

determines the action for the next phase. Input includes the local state of the environment and states of the memory and output systems. The following action phase carries out the action determined in the previous computation phase. Local environmental observations may be needed. The task is complete when the desired goal is reached. Additional details including a description of the dynamics as a Feynman sum over phase paths are given elsewhere¹.

¹P. Benioff, *Phys. Rev. A* **58** 893 (1998)

²L. K. Grover, in *Proceedings of 28th Annual ACM Symposium on Theory of Computing* ACM Press New York 1996, p. 212; *Phys. Rev. Letters*, **79** 325 (1997); G. Brassard, *Science* **275**, 627 (1997).

Study of a simple example of a search task was begun in which a quantum robot searches a 2-D region R of $N \times N$ sites to determine the site location of a particle. The idea here is to exploit quantum mechanical parallelism by putting the memory system in a superposition state

$$= \frac{1}{N} \sum_{X,Y=0}^{N-1} |X,Y\rangle .$$

Here each state $|X,Y\rangle$ corresponds to a specific site of R to examine for the presence or absence of the particle. Since all sites of R are searched in parallel and coherently, the idea is to see if Grover's Algorithm² can be used to efficiently process the memory of the returned quantum robot to determine the location of the particle. If so one would have an example of a task that can be done more efficiently by a quantum robot than by any classical robot. During 1999 work had not progressed sufficiently to see if this was possible.

d.8. The Representation of Natural Numbers in Quantum Mechanics (P. Benioff)

Work was begun on conditions that a physical system must have in order that states of the system represent the natural numbers (nonnegative integers). That states of many physical systems satisfy the conditions is clear from the existence of classical computers and the projected existence of simple quantum computers¹. However there are also many systems with no states suitable for representing the numbers.

Necessary conditions that must be satisfied are based on the relation

$$s = \sum_{j=1}^L k^{j-1} s_j$$

between a string \underline{s} of L digits with k values 0,1,...k-1 and the corresponding number s. The goal is to give,

for a quantum system with L components, conditions that a tensor product basis state of the form $|\underline{s} = \prod_a |s_a\rangle$ must satisfy so that the above equation is satisfied.

Work has progressed on describing necessary conditions for such a system. Some of them are the usual ordering conditions on the set A of L labels and on the k basis states for each component system. The new part is a dynamical condition based on these orderings. This is that there must exist operations that are *efficiently implementable physically* that correspond to the operations of addition of k^{j-1} for $j = 1, 2, \dots, L$. Work is progressing on describing these conditions in more detail.

¹L. Vandersypen *et al.*, Los Alamos Archives Report No. quant-ph/9910075; J. Ahn, T. Weinacht, and P. Bucksbaum, Science **287**, 463-465, (2000).

E. OTHER ACTIVITIES

e.1. International Workshop on Understanding Deconfinement in QCD (C. D. Roberts, D. Blaschke,* and F. Karsch†)

In partnership with D. Blaschke (University of Rostock) and F. Karsch (University of Bielefeld), C.D. Roberts organized an International Workshop on "Understanding Deconfinement in QCD" at the European Centre for Theory, Trento, Italy, 1-13 March 1999. The workshop's primary focus was QCD at nonzero baryon density, although nonzero temperature was also considered. Nonzero baryon density is a domain of QCD that is inaccessible with current lattice-QCD simulation algorithms because the integrand in the functional integral is complex. Hence this direct, quantitative approach cannot presently address questions as important as whether a quark-gluon plasma exists in the interior of dense astrophysical objects. The workshop brought together approximately sixty

physicists whose specializations ranged from lattice-QCD and matrix models to Dyson-Schwinger equations and phenomenological models. The presentations described current research on overcoming the lattice-QCD problems at nonzero baryon density and the predictions of the more phenomenological approaches, which can already explore this domain. Representatives of the large CERN experimental collaborations were also present and gave up-to-date summaries of their results. We gathered written contributions together and published them in a proceedings volume¹, which should prove useful because much new material was presented at the meeting.

*University of Rostock, Germany, †University of Bielefeld, Germany

¹Proceedings of the International Workshop on Understanding Deconfinement in QCD, eds. D. Blaschke, F. Karsch, and C.D. Roberts (World Scientific, Singapore, 2000)

e.2. Theory Institute on Advanced Computational Methods in the Nuclear Many-body Problem (S. C. Pieper, R. Roncaglia, K. Varga, and R. B. Wiringa)

A Theory Institute on "Advanced Computational Methods in the Nuclear Many-body Problem" was held during the week of August 2-6, 1999. The Institute brought together 45 theorists, including 15 postdocs and graduate students, representing 24 universities and laboratories, both domestic and foreign. A total of 28 talks were presented, on subjects ranging from the nucleon-nucleon interaction at the quark level to large-scale shell model calculations, and from low-energy astrophysical reactions to GeV electron scattering. The primary focus was on recent developments in computational methods that are used for microscopic

nuclear many-body calculations, including Fadde'ev-Yakubovsky, resonating group, coupled-cluster, correlated-basis, and quantum Monte Carlo methods. The meeting included an excursion to downtown Chicago to see the "Cows on Parade" exhibition (www.cowsonparade.net) and an outdoor symphony concert. The program of Theory Institutes at Argonne has been sponsored by Frank Fradin, the Associate Laboratory Director for Physical, Biological and Computational Sciences, for ten years; this is the largest nuclear physics workshop in the series to date.

e.3. Twelfth Annual Midwest Nuclear Theory Get-Together (R. B. Wiringa)

The Theory Group hosted the Twelfth Annual Midwest Nuclear Theory Get-Together on September 24 and 25, 1999. Nuclear theorists from a number of midwest universities get together every fall to find out what different people and groups in the region are working on. The organizational duties rotate among the participants, but Argonne has become the regular meeting place by virtue of its facilities and central location. The organizer for 1999 was Bill Friedman of the University of Wisconsin. The meeting provides a good chance for students to broaden their horizons and get some practical speaking experience in a friendly

atmosphere. The format is very informal, with an agenda of talks being volunteered at the beginning of the meeting. This year we had the largest attendance ever: 30 faculty, postdocs, and students from twelve different universities in Illinois, Indiana, Iowa, Michigan, Minnesota, Missouri, Ohio, and Wisconsin, along with the Argonne staff. Some 28 presentations were made over Friday afternoon and Saturday morning. Topics included light-front and effective field theories, QCD, quantum Monte Carlo methods, pionic fusion, relativistic heavy-ion collisions, and nuclear astrophysics. A good time was had by all.

